PIKfyve regulates $Ca_V1.2$ degradation and prevents excitotoxic cell death

Fuminori Tsuruta, Eric M. Green, Matthieu Rousset, and Ricardo E. Dolmetsch

Department of Neurobiology, Stanford University School of Medicine, Stanford, CA 94305

Voltage-gated Ca^{2+} channels (VGCCs) play a key role in neuronal signaling but can also contribute to cellular dysfunction and death under pathological conditions such as stroke and neurodegenerative diseases. We report that activation of *N*-methyl-D-aspartic acid receptors causes internalization and degradation of $Ca_V1.2$ channels, resulting in decreased Ca^{2+} entry and reduced toxicity. $Ca_V1.2$ internalization and degradation requires binding to phosphatidylinositol 3-phosphate 5-kinase (PIKfyve), a lipid kinase which generates phosphatidylinositol (3,5)-bisphosphate (PtdIns(3,5)P_2) and regulates endosome and lysosome function. Sustained activation of glutamate receptors recruits PIKfyve to $Ca_V1.2$ channels, increases cellular levels of PtdIns(3,5)P_2, and promotes targeting of $Ca_V1.2$ to lysosomes. Knockdown of PIKfyve prevents $Ca_V1.2$ degradation and increases neuronal susceptibility to excitotoxicity. These experiments identify a novel mechanism by which neurons are protected from excitotoxicity and provide a possible explanation for neuronal death in diseases caused by mutations that affect PtdIns(3,5)P_2 regulation.

Introduction

There is increasing evidence that Ca^{2+} overload and excitotoxicity are central players in a wide variety of neurological diseases, including stroke and Parkinson's and Alzheimer's diseases (Orrenius et al., 2003; Dong et al., 2006). Glutamate receptors and voltage-gated Ca^{2+} channels (VGCCs) are the main sources of Ca^{2+} influx in neurons and contribute significantly to pathological Ca^{2+} elevations. To prevent Ca^{2+}-induced damage, neurons have evolved a variety of feedback pathways that limit Ca^{2+} influx during periods of excessive extracellular glutamate or intense electrical activity (Stotz and Zamponi, 2001; Budde et al., 2002; Davis and Linn, 2003; Green et al., 2007; Jarvis and Zamponi, 2007). Among the most important of these feedback pathways is the internalization of Ca^{2+} channels, which are the main sources of Ca^{2+} in excitable cells. Glutamate receptors are internalized after tetanic stimulation or bath treatment with glutamate (Derkach et al., 2007; Lau and Zukin, 2007), but it is not known whether this type of stimulation also causes internalization of VGCCs.

VGCCs are classified according to their biophysical properties and susceptibility to pharmacological blockers. L-type VGCCs (LTCs) have a large persistent current that makes them a large source of intracellular Ca^{2+} (Tsien et al., 1988; Catterall, 2000). $Ca_V1.2$ is the most abundant LTC in the mammalian brain and is expressed in the spines, dendritic shafts, and cell bodies of most neurons in the brain. Several functions have been described for $Ca_V1.2$, including roles in gene expression, dendritic arborization, survival, and synaptic plasticity (Westenbroek et al., 1990; Hell et al., 1993; Catterall, 2000; Calin-Jageman and Lee, 2008). Ca^{2+} influx through $Ca_V1.2$ also contributes to neuronal death during ischemia, and LTC blockers have been shown to decrease neuronal death in models of stroke (Korenkov et al., 2000; Schurr, 2004).

The number of LTCs on the cell surface is altered under many physiological and pathological conditions. During aging and in Alzheimer's disease, there is an increase in the number of cell surface LTCs that is associated with neuronal dysfunction (Disterhoft et al., 1994; Haase et al., 1996; Thibault and Landfield,

Correspondence to Ricardo E. Dolmetsch: ricardo.dolmetsch@stanford.edu

M. Rousset's present address is Centre de Recherche de Biochimie Macromoleculaire–Centre National de la Recherche Scientifique Unité Mixte de Recherche 5237, Institut National de la Santé et de la Recherche Médicale, Université Montpellier I, Université Montpellier II, 34293 Montpellier, France.

Abbreviations used in this paper: ANOVA, analysis of variance; GAPDH, glyceraldehyde-3-phosphate dehydrogenase; LAMP, lysosomal-associated membrane protein; LTC, L-type VGCC; NMDA, *N*-methyl-D-aspartic acid; PIKfyve, phosphatidylinositol 3-phosphate 5-kinase; PtdIns(3,5)P_2, phosphatidylinositol (3,5)-bisphosphate; ROI, region of interest; shRNA, short hairpin RNA; VGCC, voltage-gated Ca^{2+} channel.

The Rockefeller University Press $30.00
J. Cell Biol. Vol. 187 No. 2 279–294
www.jcb.org/cgi/doi/10.1083/jcb.200903028

1996; Coon et al., 1999). Studies in animals and humans have reported that LTC blockers can improve performance on memory tasks (for review see Thibault et al., 2007). In addition, a developmentally regulated increase in $Ca_V1.2$ levels could lead to cell death in Parkinson's disease (Day et al., 2006; Chan et al., 2007). However, despite the importance of LTCs in neuronal pathology, the mechanisms that control their expression and trafficking are not well understood.

Phosphatidylinositol (3,5)-bisphosphate (PtdIns(3,5)P_2) is a rare phospholipid that is found in endosomal membranes and is generated by the activity of a lipid kinase called phosphatidylinositol 3-phosphate 5-kinase (PIKfyve; mammals) or Fab1 (yeast; Michell et al., 2006). PIKfyve/Fab1 is critically important for the regulation of membrane trafficking and for the function of endosomes and lysosomes. Fab1 mutants have enlarged vacuoles and defects in multivesicular body invagination and vacuole acidification (Gary et al., 1998; Odorizzi et al., 1998; Efe et al., 2005). Genetic disruption of Fab1 is lethal in model organisms, and inhibition of PIKfyve leads to the enlargement of endosomes and formation of vacuoles in cells in culture (Ikonomov et al., 2001; Nicot et al., 2006; Rusten et al., 2006; Rutherford et al., 2006).

Recently, it has been shown that mutations that alter the production of PtdIns(3,5)P_2 cause severe neuronal defects in both mice and in humans. Mutations in mouse Fig4 and Vac14, two proteins which regulate PIKfyve (Duex et al., 2006; Sbrissa et al., 2007; Botelho et al., 2008), reduce PtdIns(3,5)P_2 levels and lead to ataxia and neuronal death (Chow et al., 2007; Zhang et al., 2007). In addition, mutations in other proteins that control PtdIns(3,5)P_2 levels cause neuronal and muscular diseases, including myotubular myopathy, amyotrophic lateral sclerosis, and Charcot-Marie-Tooth disease (Nicot and Laporte, 2008). This raises the question of why, despite the ubiquitous production of PtdIns(3,5)P_2 in cells, mutations in this pathway preferentially affect excitable cells like neurons and myocytes.

In this study, we report that sustained glutamate exposure causes internalization and degradation of $Ca_V1.2$ in cortical neurons. Using a proteomic screen, we identify PIKfyve as a $Ca_V1.2$-binding protein, and we show that this protein binds to $Ca_V1.2$ upon activation of glutamate receptors. PIKfyve is required for both internalization and degradation of the channel, and loss of PIKfyve increases the susceptibility of neurons to cell death in response to activation of glutamate receptors. Our study suggests that PIKfyve-dependent channel degradation is essential to prevent Ca^{2+}-induced toxicity in neurons. These experiments provide a direct link between Ca^{2+} signaling and PIKfyve and help to explain why defects in PtdIns(3,5)P_2 signaling are deleterious to cells that are susceptible to excitotoxicity such as neurons and myocytes.

Results

Glutamate stimulation promotes $Ca_V1.2$ internalization and degradation

Ischemia and stroke cause neuronal death by triggering excess release of glutamate into the extracellular space, which activates Ca^{2+} influx through *N*-methyl-D-aspartic acid (NMDA) receptors and VGCCs and leads to Ca^{2+}-induced toxicity (Schurr, 2004). Although it is known that activation of glutamate receptors causes internalization of AMPA and NMDA receptors (Derkach et al., 2007; Lau and Zukin, 2007), little is known about the effect of excess glutamate on the cell surface expression of VGCCs. To determine whether glutamate receptors regulate the number of $Ca_V1.2$ channels on the cell surface, we used an assay that we previously developed to measure the surface levels of $Ca_V1.2$ channels in primary neurons (Green et al., 2007). We introduced $Ca_V1.2$ channels containing both an intracellular YFP and an extracellular HA epitope into primary cortical neurons and used anti-HA antibodies to label channels on the cell surface. Because the HA antibodies do not cross the cell membrane, the ratio of the anti-HA to YFP fluorescence provides a quantitative measurement of the proportion of channels on the plasma membrane.

Stimulation with 50 µM glutamate led to a 60% decrease in the proportion of $Ca_V1.2$ channels on the cell surface, indicating that a significant proportion of $Ca_V1.2$ channels are internalized relatively rapidly by a large dose of glutamate (Fig. 1, A and B). To provide independent evidence that activation of glutamate receptors causes loss of cell surface $Ca_V1.2$ channels, we used Ca^{2+} imaging to measure Ca^{2+} influx in neurons before and after treatment with high concentrations of glutamate. Treatment with 50 µM glutamate for 10 min caused a significant decrease in the intracellular Ca^{2+} rise induced by depolarization. This decrease could be observed both at the population level and in single cells (Fig. 1 C). Together, these experiments suggest that relatively prolonged activation of glutamate receptors causes loss of $Ca_V1.2$ channels on the cell membrane.

Because prolonged treatment with glutamate can cause excitotoxicity in neurons, we next investigated whether loss of $Ca_V1.2$ channels was correlated with cell death in neurons. We treated neurons with 10, 50, or 100 µM glutamate for 3, 10, or 30 min or 10 h and measured cell death 10 h later by counting pyknotic nuclei, measuring MAP2 levels in dendrites, or using TUNEL staining (Fig. S1). Although treatment with 50 or 100 µM glutamate for 30 min or 10 h caused substantial apoptotic cell death, stimulation with 50 µM glutamate for 10 min (conditions which cause channel internalization) did not lead to cell death. This suggests that $Ca_V1.2$ internalization is not correlated with cell death and therefore is more likely to be a cellular response to a potentially cytotoxic stimulus.

In a previous study, we found that stimulation of neurons using relatively mild depolarizing stimuli to activate $Ca_V1.2$ channels caused a reversible loss of cell surface $Ca_V1.2$ channels (Green et al., 2007). Under these conditions, $Ca_V1.2$ channels are returned to the membrane rapidly after restoration of the resting membrane potential. To investigate whether activation of glutamate receptors also led to reversible loss of $Ca_V1.2$ channels from the cell membrane, we stimulated neurons with 50 µM glutamate for 10 min and then returned the cells to resting conditions for 20 min before measuring cell surface channels. In contrast to our previous findings (Green et al., 2007), we observed no recovery of $Ca_V1.2$ channels on the cell membrane 20 min after treatment with 50 µM glutamate (Fig. 1 D),

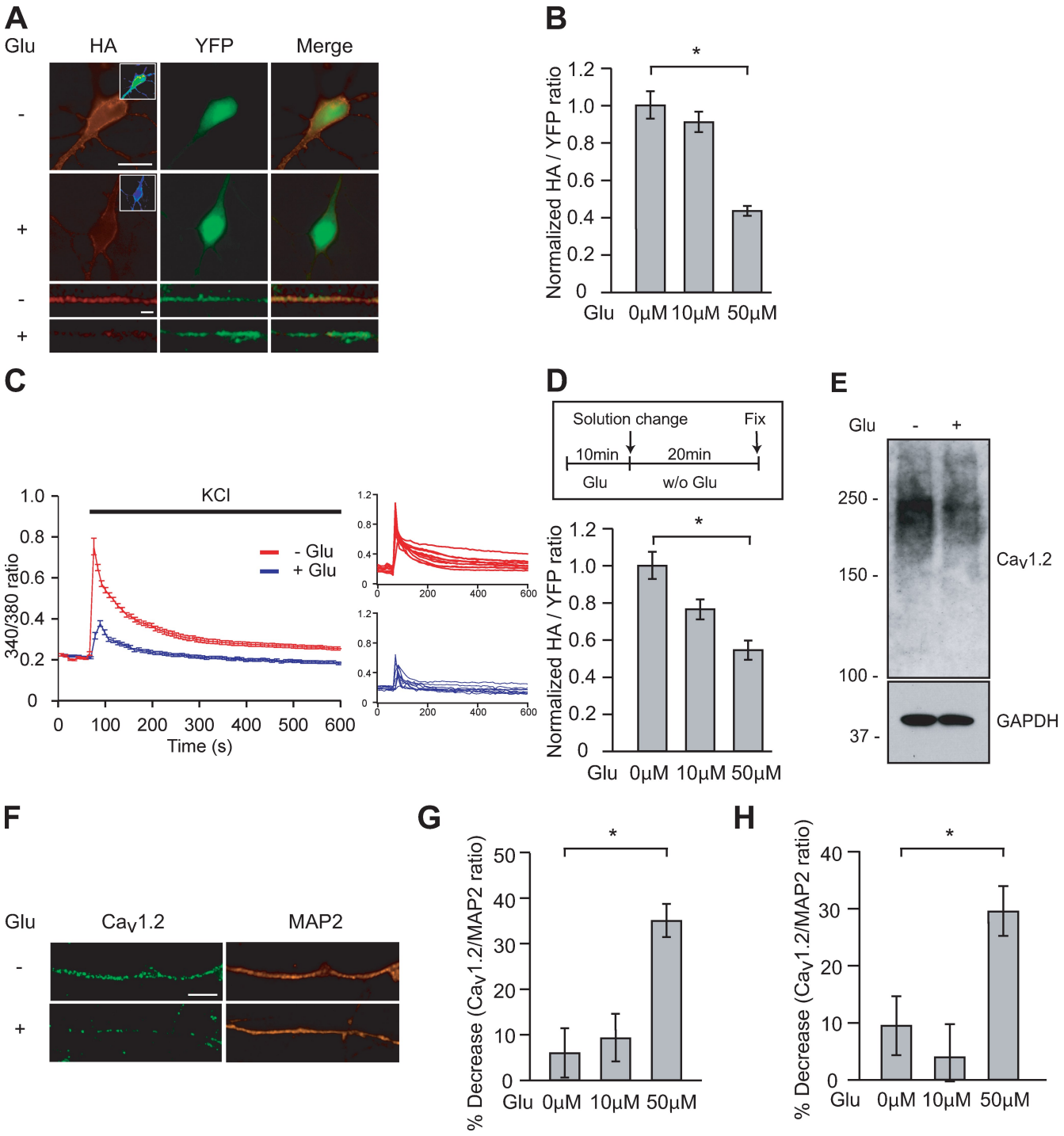

Figure 1. **Activation of glutamate receptors promotes $Ca_V1.2$ internalization and degradation.** (A) Cortical neurons expressing YFP-HA-$Ca_V1.2$ channels were treated with 50 μM glutamate (Glu) for 10 min and stained with anti-HA antibodies without permeabilization. The top six panels show staining in neuronal cell bodies; to distinguish changes in staining intensity more easily, the insets show the same images using a rainbow color scheme. The bottom six panels show staining in dendrites. (B) Quantification of data from A ($n = 30$; mean ± SEM; *, $P < 0.0001$ by Student's *t* test). (C) Ratiometric measurement of intracellular Ca^{2+} in neurons incubated in the absence or presence of 50 μM glutamate for 10 min and depolarized with 67 mM KCl ($n = 50$; mean ± SEM). The panel on the left shows the mean Ca^{2+} responses, and the inset graphs show individual traces. (D) A 20-min recovery period after glutamate stimulation for 10 min did not lead to recovery of YFP-HA-$Ca_V1.2$ surface levels ($n = 30$; mean ± SEM; *, $P < 0.0001$ by Student's *t* test). (E) Cortical neurons were incubated with 50 μM glutamate for 15 min and analyzed by Western blotting with anti-$Ca_V1.2$ and anti-GAPDH antibodies ($n = 3$). Molecular mass is indicated in kilodaltons. (F) Cortical neurons were stimulated with glutamate for 10 min and then stained with anti-$Ca_V1.2$ and MAP2 antibodies to show changes in endogenous $Ca_V1.2$ in dendrites after stimulation. (G) Ratio of $Ca_V1.2$ to MAP2 fluorescence on neuronal dendrites treated as in F ($n = 200$ dendrites; mean ± SEM; *, $P < 0.0001$ by Student's *t* test). (H) Endogenous $Ca_V1.2$ surface levels 20 min after glutamate stimulation ($n = 30$; mean ± SEM; *, $P < 0.0001$ by Student's *t* test). Bars: (A, top) 20 μm; (A, bottom) 3 μm; (F) 5 μm.

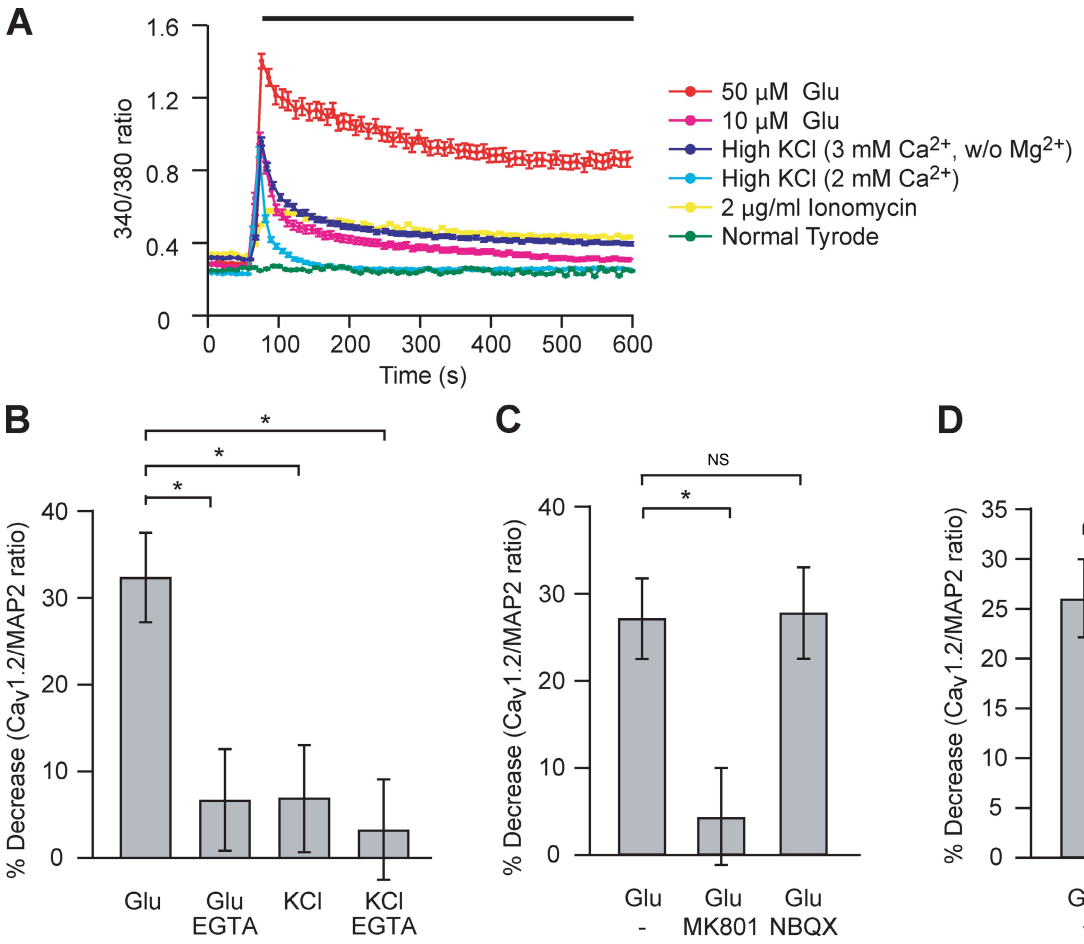

Figure 2. **NMDA receptors mediate $Ca_V1.2$ degradation in a Ca^{2+}-dependent manner.** (A) Ratiometric measurement of $[Ca^{2+}]_i$ in neurons treated with glutamate (Glu), 67 mM KCl, or 2 µg/ml ionomycin (n = 100; mean ± SEM). (B) Neurons were stimulated with 50 µM glutamate or 67 mM KCl for 10 min in the absence or presence of 2.5 mM EGTA. The graph shows the percent decrease in the ratio of $Ca_V1.2$ to MAP2 fluorescence on dendrites (n = 200 dendrites; mean ± SEM; *, P < 0.01 by one-way analysis of variance [ANOVA] with the Newman-Keuls multiple comparison test). (C) Change in the surface expression of $Ca_V1.2$ in dendrites of neurons treated with 50 µM glutamate for 10 min in the presence of 10 µM MK801 or 10 µM NBQX (n = 200 dendrites; mean ± SEM; *, P < 0.01 by one-way ANOVA). (D) Change in the surface expression of $Ca_V1.2$ in dendrites of neurons treated with 50 µM glutamate for 10 min in the presence of 300 µM DL-AP3 (n = 200 dendrites; mean ± SEM; NS by Student's t test).

suggesting that activation of glutamate receptors leads to a permanent loss of $Ca_V1.2$ channels on the cell surface.

To determine whether the loss of $Ca_V1.2$ from the cell membrane was caused by channel degradation, we measured $Ca_V1.2$ levels in neurons either by Western blotting or by immunofluorescence. We stimulated neurons with 50 µM glutamate and used SDS-PAGE and anti-$Ca_V1.2$ antibodies to detect endogenous $Ca_V1.2$ channels (Fig. S2, A–C). We found that this treatment caused a reproducible decrease in the levels of $Ca_V1.2$ relative to a glyceraldehyde-3-phosphate dehydrogenase (GAPDH) internal control (Fig. 1 E), suggesting that $Ca_V1.2$ was degraded after activation of glutamate receptors. To provide further evidence of glutamate-induced $Ca_V1.2$ degradation, we used immunocytochemistry to detect $Ca_V1.2$ channels in cultures of neurons before and after treatment with 50 µM glutamate for 10 min. Glutamate caused a 35% loss of $Ca_V1.2$ immunoreactivity from the dendrites and a redistribution of the channel to a region around the cell nucleus (Fig. 1, F and G; and Fig. S2 D). This decrease in the levels of the endogenous channel was not reversed by a 20-min incubation in glutamate-free media (Fig. 1 H), providing additional evidence for $Ca_V1.2$ channel degradation.

$Ca_V1.2$ degradation depends on NMDA receptors

We next investigated whether $Ca_V1.2$ degradation depended on the elevation of the intracellular Ca^{2+} concentration ($[Ca^{2+}]_i$) and on the activation of specific types of glutamate receptors. We used Fura-2 to measure $[Ca^{2+}]_i$ and found that treatment with 50 µM glutamate, which causes channel degradation, caused a $[Ca^{2+}]_i$ rise that was significantly greater than treatment with 10 µM glutamate, 67 mM KCl, or 2 µg/ml ionomycin (Fig. 2 A). To determine whether Ca^{2+} influx was required for glutamate-dependent $Ca_V1.2$ degradation, we stimulated cells with 50 µM glutamate in media with reduced extracellular Ca^{2+} and found that this completely prevented $Ca_V1.2$ degradation (Fig. 2 B). This indicates that Ca^{2+} influx across the membrane is required for this process.

Glutamate stimulation elevates $[Ca^{2+}]_i$ by a variety of mechanisms, including activation of Ca^{2+}-permeable AMPA and NMDA

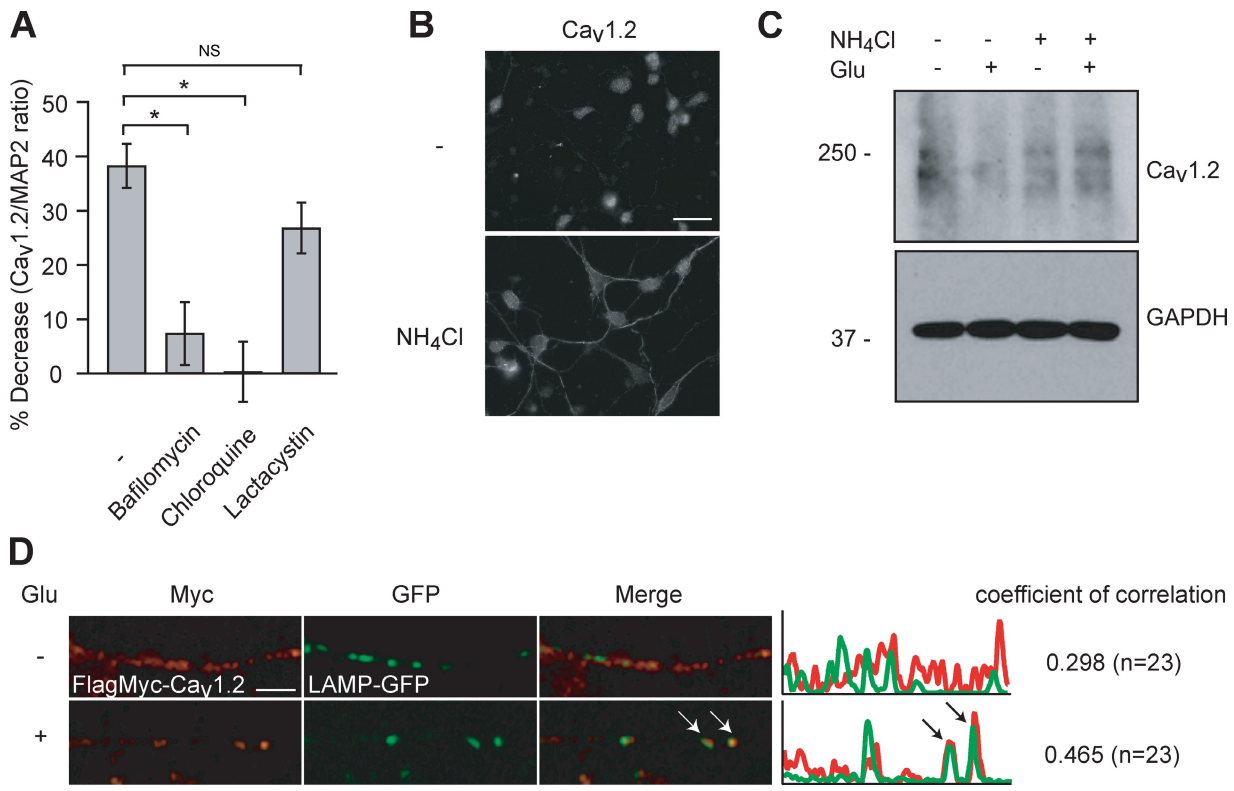

Figure 3. **Glutamate-induced $Ca_V1.2$ degradation is mediated by lysosomes.** (A) Neurons were incubated with 100 µM chloroquine or 100 nM bafilomycin for 3 h or with 2 µM lactacystin for 1 h and then stimulated with 50 µM glutamate for 10 min. The graph shows the percent decrease in the ratio of $Ca_V1.2$ to MAP2 fluorescence on dendrites (n = 200 dendrites; mean ± SEM; *, $P < 0.001$ by one-way ANOVA). (B) Cortical neurons (3 d in vitro) were treated with or without 30 mM NH_4Cl for 3 h and then analyzed by immunocytochemistry with anti-$Ca_V1.2$ antibodies. Representative images are shown. (C) Cortical neurons were treated with or without 30 mM NH_4Cl for 30 min and then incubated with 50 µM glutamate for 15 min and subjected to immunoblot analysis with anti-$Ca_V1.2$ and anti-GAPDH antibodies. Molecular mass is indicated in kilodaltons. (D) Fluorescent images of neurons expressing Flag-Myc-$Ca_V1.2$ and LAMP-GFP. Cells were stained with anti-Myc and anti-GFP antibodies before and after treatment with 50 µM glutamate (Glu) for 15 min (n = 5 neurons and 23 dendrites). The arrows show colocalization of $Ca_V1.2$ and the lysosomal marker LAMP-GFP. Bars: (B) 30 µm; (D) 2.5 µm.

receptors, metabotropic glutamate receptors, and indirect activation of VGCCs. To examine which of these pathways is responsible for $Ca_V1.2$ degradation, we treated neurons with 50 µM glutamate in the presence of NBQX, MK801, or DL-AP3 to block AMPA, NMDA, or metabotropic glutamate receptors, respectively. Treatment with NBQX and DL-AP3 had no effect on $Ca_V1.2$ degradation, but treatment with MK801 prevented loss of $Ca_V1.2$ from dendrites (Fig. 2, C and D), indicating that $Ca_V1.2$ degradation depends on NMDA receptors. This is in agreement with a previous study of loss of LTC currents in neurons treated with NMDA (Davis and Linn, 2003).

Glutamate-induced $Ca_V1.2$ degradation occurs via lysosomes

Glutamate-triggered $Ca_V1.2$ degradation could occur either via the lysosomal or the proteosomal pathways. To determine which pathways regulate channel degradation, we treated cells with the lysosomal inhibitors bafilomycin and chloroquine or with the proteosomal inhibitor lactacystin. Both bafilomycin and chloroquine significantly inhibited glutamate-induced $Ca_V1.2$ degradation, whereas lactacystin had no significant effect (Fig. 3 A). In addition, NH_4Cl, which prevents lysosomal acidification, caused a large increase in the number of $Ca_V1.2$ channels on the cell surface (Fig. 3 B) and reversed the glutamate-induced decrease in $Ca_V1.2$ channels (Fig. 3 C). Together, these data suggest that lysosomes play a central role in $Ca_V1.2$ channel degradation in neurons.

To provide further evidence for the importance of lysosomes in the degradation of $Ca_V1.2$, we investigated whether treatment of neurons with glutamate caused relocalization of Ca^{2+} channels to lysosomal compartments. We introduced a Flag-Myc–labeled $Ca_V1.2$ channel (Flag-Myc-$Ca_V1.2$) and a GFP fusion protein of the lysosomal-associated membrane protein (LAMP; LAMP-GFP) into neurons (Fig. S3 A). Treatment with glutamate caused a significant increase in the colocalization of $Ca_V1.2$ and LAMP-GFP in neuronal dendrites (Fig. 3 D), suggesting that the channels are targeted to lysosomes by activation of glutamate receptors.

PIKfyve associates with $Ca_V1.2$

To provide further insight into the mechanisms that underlie $Ca_V1.2$ internalization and degradation, we used a proteomic approach to identify $Ca_V1.2$-binding proteins. We expressed GST fusion proteins of the intracellular domains of $Ca_V1.2$ in Neuro2A neuroblastoma cells, immunoprecipitated the proteins, and used multidimensional mass spectrometry to identify associated proteins. GST-YFP was immunoprecipitated and analyzed in parallel as control for nonspecific protein binding. We repeated

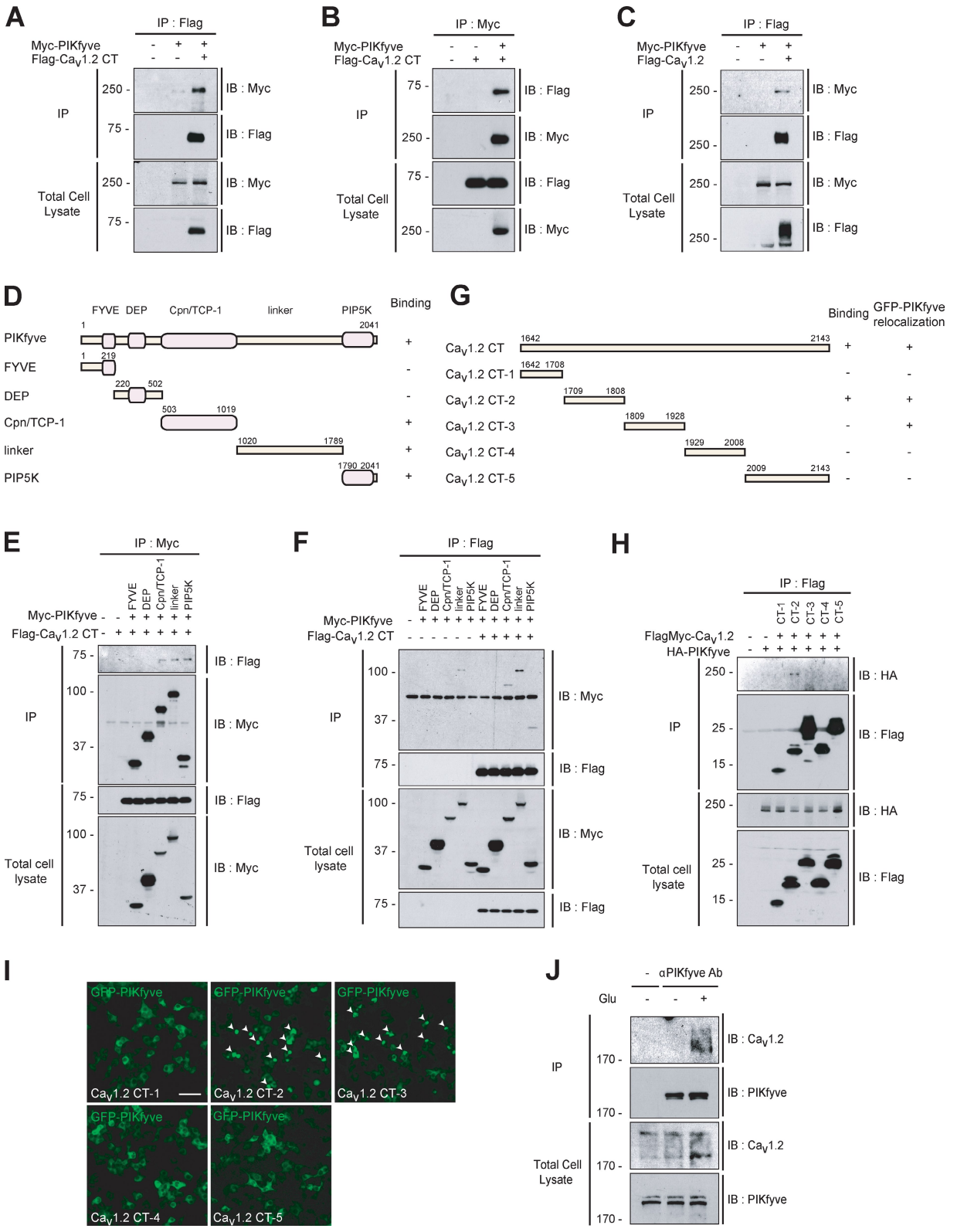

Figure 4. **PIKfyve associates with $Ca_V1.2$.** (A and B) Coimmunoprecipitation of full-length Myc-PIKfyve and of the Flag-tagged C terminus of $Ca_V1.2$ (Flag–$Ca_V1.2$ CT) coexpressed in HEK 293T cells with either anti-Flag (A) or anti-Myc (B) antibodies. (C) Coimmunoprecipitation of full-length Flag-$Ca_V1.2$ and Myc-PIKfyve in HEK 293T cells. Flag-$Ca_V1.2$ was immunoprecipitated with anti-Flag antibodies, and the immunoprecipitated material was analyzed using both Myc and Flag antibodies. (D) Schematic structure of deletion mutants of PIKfyve. (E and F) Immunoprecipitation (IP) of the deletion mutants of PIKfyve and of the C terminus of $Ca_V1.2$ expressed in HEK 293T cells. Cell lysates were subjected to immunoprecipitation with either anti-Myc (E) or anti-Flag (F) antibodies, and Western blots were analyzed to detect interacting proteins. (G) Schematic structure of deletion mutants of the C terminus of $Ca_V1.2$. (H) Coimmunoprecipitation of the Flag-Myc-$Ca_V1.2$ C terminus deletion mutants (CT-1 through CT-5) with full-length PIKfyve (HA-PIKfyve) expressed in HEK 293T cells using anti-Flag antibodies. Western blots were performed using both anti-Flag and anti-HA antibodies. (I) Coexpression of $Ca_V1.2$ CT-2 and CT-3

the experiment five times and generated a score for each $Ca_V1.2$-interacting protein that reflected the number of times that the protein bound to $Ca_V1.2$ relative to YFP (Table S1). One of the main proteins that associated with the cytoplasmic C terminus of $Ca_V1.2$ was PIKfyve, a lipid kinase which is localized in early endosomes (Fig. S3, B and C) and controls endosomal and lysosomal trafficking. Because $Ca_V1.2$ is degraded in lysosomes in response to glutamate stimulation, we investigated whether PIKfyve has a role in regulating this process.

To verify that $Ca_V1.2$ interacts with PIKfyve in cells, we introduced Myc-PIKfyve and Flag-$Ca_V1.2$ expression plasmids into HEK 293T cells, lysed the cells, and immunoprecipitated the channel using anti-Flag or anti-Myc antibodies. Immunoprecipitation of the full-length channel (Fig. 4 C) or of the cytoplasmic C terminus of the channel (Fig. 4 A) resulted in coimmunoprecipitation of full-length PIKfyve. Conversely, immunoprecipitation of PIKfyve caused coimmunoprecipitation of the $Ca_V1.2$ C terminus (Fig. 4 B). We next expressed GFP-PIKfyve and the $Ca_V1.2$ C terminus in HEK 293T cells. Expression of the $Ca_V1.2$ C terminus caused GFP-PIKfyve to form large perinuclear aggregates, providing additional evidence that these two proteins interact in cells (Fig. S3 D).

We then used deletion analysis to map the domains of PIKfyve and $Ca_V1.2$ that interact with each other. We subdivided PIKfyve into five fragments (Fig. 4 D), expressed them in HEK 293T cells, and tested their ability to interact using coimmunoprecipitation assays. The two N-terminal fragments of PIKfyve did not associate with the C terminus of $Ca_V1.2$, but the three C-terminal fragments all interacted with this channel (Fig. 4, E and F). We also subdivided the C terminus of $Ca_V1.2$ into five fragments and tested the association of these fragments with full-length PIKfyve (Fig. 4 G). We found that a domain composed of aa 1,709–1,808 of $Ca_V1.2$ (CT-2) interacted with full-length PIKfyve, whereas other regions did not (Fig. 4 H). Expression of this CT-2 fragment and the fragment immediately terminal to it (aa 1,809–1,928 or CT-3) caused GFP-PIKfyve to form perinuclear aggregates that were identical to those formed with the full C terminus of $Ca_V1.2$ (Fig. 4 I). Together, these results suggest that aa 1,709–1,808 of $Ca_V1.2$ and the C-terminal fragment of PIKfyve are required for the interaction of these two proteins. The region from aa 1,709–1,808 is highly conserved in LTCs across various species, suggesting that it is likely to define a motif that is important for channel function. Although the nature of these proteins made it impossible to purify them from bacteria to test for a direct interaction, our data are consistent with a direct interaction between the C-terminal domains of $Ca_V1.2$ and PIKfyve.

We next investigated whether $Ca_V1.2$ interacts with PIKfyve in a glutamate-dependent manner. We used anti-PIKfyve antibodies to immunoprecipitate PIKfyve from cultured neurons before and after treatment with glutamate and used anti-$Ca_V1.2$ to detect the channel by Western blotting. $Ca_V1.2$ did not associate with PIKfyve in resting cells, but in neurons stimulated with glutamate, $Ca_V1.2$ (Fig. 4 J) was reproducibly coimmunoprecipitated with PIKfyve. These data argue that endogenous $Ca_V1.2$ associates with endogenous PIKfyve and, further, that this occurs in response to activation of glutamate receptors.

Activation of glutamate receptors increases PtdIns(3,5)P_2 levels

The inducible interaction of PIKfyve with $Ca_V1.2$ under conditions of excitotoxic stress suggested that PIKfyve could be activated by glutamate receptors. To study this question, we made an intracellular sensor for PtdIns(3,5)P_2, which is the main product of PIKfyve in cells. We made a fusion protein of GFP and two copies of the GRAM domain from the phosphatase myotubularin (MTM1; Fig. 5 A), which binds to PtdIns(3,5)P_2 (Tsujita et al., 2004). We introduced this protein into neurons and, upon treatment with 50 µM glutamate, observed a marked relocalization from the cytoplasm and the nucleus to a perinuclear region (Fig. 5, B and C). This change in localization was not observed in cells expressing GFP alone, suggesting that it is specific to the GRAM-containing protein. The change in GFP-GRAM localization was only observed in neurons treated with 50 µM glutamate but not with glutamate in the presence of EGTA, elevated KCl, or ionomycin, indicating that this event occurs only under the conditions that lead to $Ca_V1.2$ degradation (Fig. 5 D).

The perinuclear localization of GFP-GRAM after glutamate treatment was very similar to that of lysosomes and late endosomes, so we explored whether GFP-GRAM relocalizes to these compartments after activation of glutamate receptors. We coexpressed in neurons GFP-GRAM and the lysosome marker LAMP-Cherry and observed a small increase in the colocalization of the two proteins after treatment with glutamate (Fig. S3 E). This indicates that PtdIns(3,5)P_2 is generated in endosomal compartments in response to glutamate receptor activation.

To provide independent evidence that activation of glutamate receptors leads to an increase in PtdIns(3,5)P_2 in neurons, we used a monoclonal antibody to detect PtdIns(3,5)P_2. This antibody is relatively specific for PtdIns(3,5)P_2, as determined by its ability to detect a decrease in PtdIns(3,5)P_2 levels in knockouts of ppk-3, the *Caenorhabditis elegans* homologue of PIKfyve (Nicot et al., 2006). Treatment of neurons with 50 µM glutamate resulted in an increase in anti-PtdIns(3,5)P_2 fluorescence, which is consistent with our earlier finding (Fig. 5 B) that glutamate leads to relocalization of the GFP-GRAM domain (Fig. 5, E and F). Together, these results provide evidence that activation of glutamate receptors leads to an increase in PtdIns(3,5)P_2 levels in neurons.

We next asked whether the increase of PtdIns(3,5)P_2 triggered by activation of glutamate receptors depends on PIKfyve activity. We made short hairpin RNAs (shRNAs) that target PIKfyve (shPIKfyve) and two PIKfyve constructs that contain silent mutations in the region recognized by the shRNA that could be

caused aggregation of GFP-PIKfyve in a structure close to the nucleus. Arrowheads show PIKfyve aggregates that are formed when PIKfyve is coexpressed with C-terminal fragments of $Ca_V1.2$. (J) Coimmunoprecipitation of endogenous $Ca_V1.2$ and PIKfyve from neurons before or after treatment with 50 µM glutamate for 5 min (n = 3). (A–C, E, F, H, and J) Molecular mass is indicated in kilodaltons. Ab, antibody; IB, immunoblot. Bar, 50 µm.

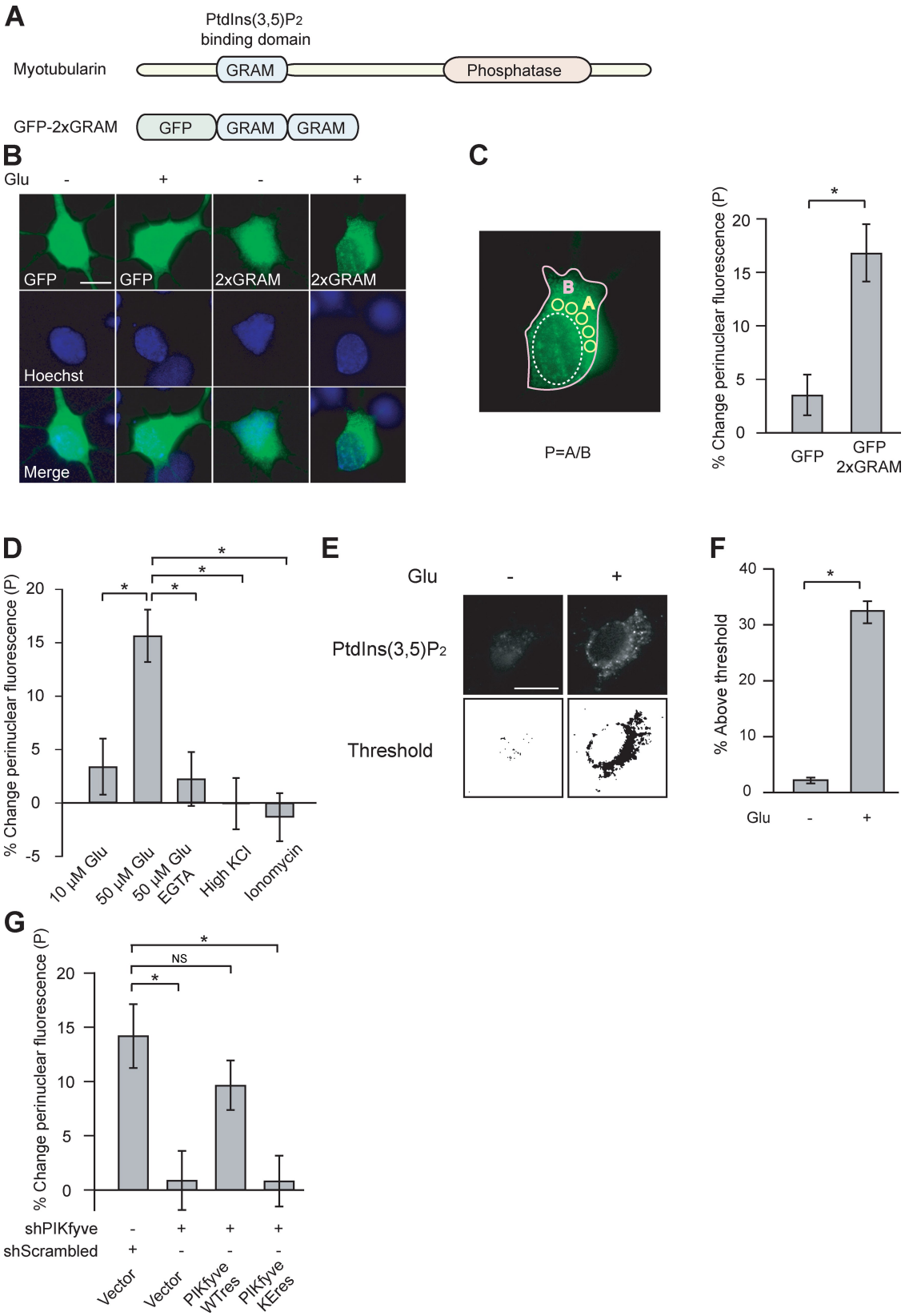

Figure 5. **Activation of glutamate receptors increases PtdIns(3,5)P$_2$ levels.** (A) Structure of myotubularin and of the GFP–2× GRAM reporter protein. (B) Fluorescent images expressing either GFP alone or the GFP–2× GRAM reporter before and after treatment with 50 µM glutamate (Glu) for 10 min. (C) Changes in perinuclear fluorescence observed in cells expressing GFP or GFP–2× GRAM after treatment with glutamate (n = 60 cells; 300 ROIs; mean ± SEM; *, P < 0.0001 by Student's t test). The areas targeted to quantify perinuclear localization are indicated in the illustration. The pink line indicates the edge of the cell, the dashed line indicates the nucleus, and the small yellow circles indicate perinuclear regions. (D) Change in perinuclear GFP–2× GRAM fluorescence before and after various types of stimulation, as indicated in Fig. 2 A (n = 60 cells; 300 ROIs; mean ± SEM; *, P < 0.001 by one-way

used to restore PIKfyve expression in the presence of the shRNAs (wild type [PIKfyve WTres] and kinase negative [PIKfyve KEres]). shPIKfyve reduced the expression of PIKfyve in HEK 293T cells but not of the shRNA-resistant proteins, as measured by Western blotting of Myc-tagged proteins (Fig. S4 A). In addition, shPIKfyve caused a dramatic increase in the number and size of vacuoles in NIH3T3 cells that was suppressed by the introduction of PIKfyve WTres but not of PIKfyve KEres (Fig. S4, B and C), indicating that these shRNAs also reduce the expression of the endogenous proteins. To determine whether PIKfyve generates PtdIns(3,5)P_2 in response to glutamate, we introduced shPIKfyve into neurons, stimulated the cells with 50 µM glutamate, and measured PtdIns(3,5)P_2 production using the GFP-GRAM protein. Introduction of shPIKfyve eliminated the relocalization of GFP-GRAM to the perinuclear region, suggesting that it also eliminated the production of PtdIns(3,5)P_2 (Fig. 5 G). Interestingly, we observed relatively few vacuoles in most neurons expressing the shPIKfyve under resting conditions, suggesting that PIKfyve activity is relatively low in resting neurons (Fig. S4 D). Introduction of a PIKfyve WTres along with shPIKfyve restored the relocalization of the GRAM domain to the perinuclear region in response to glutamate, whereas the PIKfyve KEres domain did not rescue the effects of shPIKfyve on the localization of the GFP-GRAM reporter. Together, these results provide evidence that activation of glutamate receptors leads to increases in PtdIns(3,5)P_2 levels in neurons and that this is mediated by PIKfyve.

PIKfyve regulates glutamate-dependent $Ca_V1.2$ internalization and degradation

Because PIKfyve regulates endosome trafficking, we next investigated whether it contributes to the glutamate-dependent internalization of $Ca_V1.2$ channels. We transfected neurons with shPIKfyve together with YFP-HA-$Ca_V1.2$ and measured the surface levels of $Ca_V1.2$ after stimulation with glutamate. Knockdown of PIKfyve significantly suppressed glutamate-dependent $Ca_V1.2$ internalization (Fig. 6, A and B), whereas a scrambled control shRNA (shScrambled) had no effect, suggesting that PIKfyve controls $Ca_V1.2$ levels on the cell surface. To determine whether PIKfyve also regulates degradation of endogenous $Ca_V1.2$, we introduced shPIKfyve into neurons and measured the amount of $Ca_V1.2$ channel in dendrites using anti-$Ca_V1.2$ antibodies (Fig. 6, C and D). shPIKfyve significantly decreased the degradation of $Ca_V1.2$ in neurons treated with glutamate compared with shScrambled. Introduction of PIKfyve WTres restored the glutamate-dependent degradation of $Ca_V1.2$, whereas PIKfyve KEres had no effect. Thus, PIKfyve seems to be required both for $Ca_V1.2$ internalization and degradation in response to increases in glutamate. Because the main product of PIKfyve is PtdIns(3,5)P_2, we asked whether PtdInd(3,5)P_2 was necessary for glutamate-induced $Ca_V1.2$ degradation. We overexpressed the phosphatase MTM1, which dephosphorylates PtdIns(3,5)P_2 at the 3 position, and measured dendritic $Ca_V1.2$ levels in neurons. Expression of MTM1 reduced glutamate-induced $Ca_V1.2$ degradation in dendrites (Fig. S5, A and B), providing additional evidence that PIKfyve and PtdInd(3,5)P_2 help mediate $Ca_V1.2$ degradation.

We next investigated whether the interaction of PIKfyve with the C terminus of $Ca_V1.2$ was important for glutamate-dependent $Ca_V1.2$ degradation. We generated a Myc-$Ca_V1.2$ channel that lacks the C-terminal PIKfyve-binding site ($Ca_V1.2$ ΔCT), introduced it into neurons, and measured its degradation after activation of glutamate receptors. Although the wild-type channels were efficiently degraded by activation of glutamate receptors, the levels of $Ca_V1.2$ ΔCT channels were not significantly reduced (Fig. 6, E and F), suggesting that binding of $Ca_V1.2$ to PIKfyve is required for $Ca_V1.2$ degradation in response to the activation of glutamate receptors.

Finally, we tested whether PIKfyve regulates the targeting of $Ca_V1.2$ channels to lysosomes after activation of glutamate receptors. We introduced LAMP-GFP and Myc-$Ca_V1.2$ into neurons along with shPIKfyve or shScrambled constructs and then treated cells with glutamate. We measured the colocalization of $Ca_V1.2$ and LAMP by calculating the coefficient of correlation between $Ca_V1.2$ and LAMP in cells. Treatment with glutamate caused a loss of diffuse $Ca_V1.2$ staining and the appearance of Myc-$Ca_V1.2$ puncta, some of which colocalized with LAMP-GFP, giving rise to an increase in the coefficient of correlation between the two images. Knockdown of PIKfyve substantially reduced the colocalization of $Ca_V1.2$ and LAMP after activation of glutamate receptors (Fig. 6 G), supporting the idea that $Ca_V1.2$ channels are trafficked to lysosomes after treatment with glutamate in a manner that depends on PIKfyve.

PIKfyve protects neurons against excitotoxic cell death

Under conditions of stroke and anoxia, glutamate is a potent excitotoxic agent that acts by increasing intracellular Ca^{2+} levels both through NMDA receptors and through LTCs (Schurr, 2004). We initially characterized the contribution of different Ca^{2+} channels to glutamate-triggered excitotoxicity in our cells by treating neurons for 30 min with 50 µM glutamate in the presence of blockers for NMDA receptors (MK801), AMPA receptors (NBQX), LTCs (nimodipine), P/Q-type VGCCs (agatoxin IVA), N-type VGCCs (ω-conotoxin GVIA), and R-type VGCCs (SNX482) and measuring cell death 10 h later (Fig. 7, A and B). As expected, the NMDA receptor MK801 blocked ∼80% of the cell death, the AMPA receptors and LTC blockers reduced cell death ∼25%, and the other channel blockers had essentially no effect on glutamate-induced toxicity. This indicates that although NMDA receptors are the primary triggers of excitotoxicity, both LTCs and AMPA receptors also play a role in this process.

ANOVA). (E) Cortical neurons stained with anti-PtdIns(3,5)P_2 antibodies before and after treatment with 50 µM glutamate for 10 min. (F) Quantification of the data in D showing an increase in PtdIns(3,5)P_2 levels in perinuclear regions (n = 100; mean ± SEM; *, $P < 0.0001$ by Student's t test). (G) Change in perinuclear GFP–2× GRAM fluorescence in neurons containing either shPIKfyve or shScrambled along with either a control vector or PIKfyve WTres or PIKfyve KEres after treatment with 50 µM glutamate (n = 60 cells; 300 ROIs; mean ± SEM; *, $P < 0.01$ by one-way ANOVA). Bars, 10 µm.

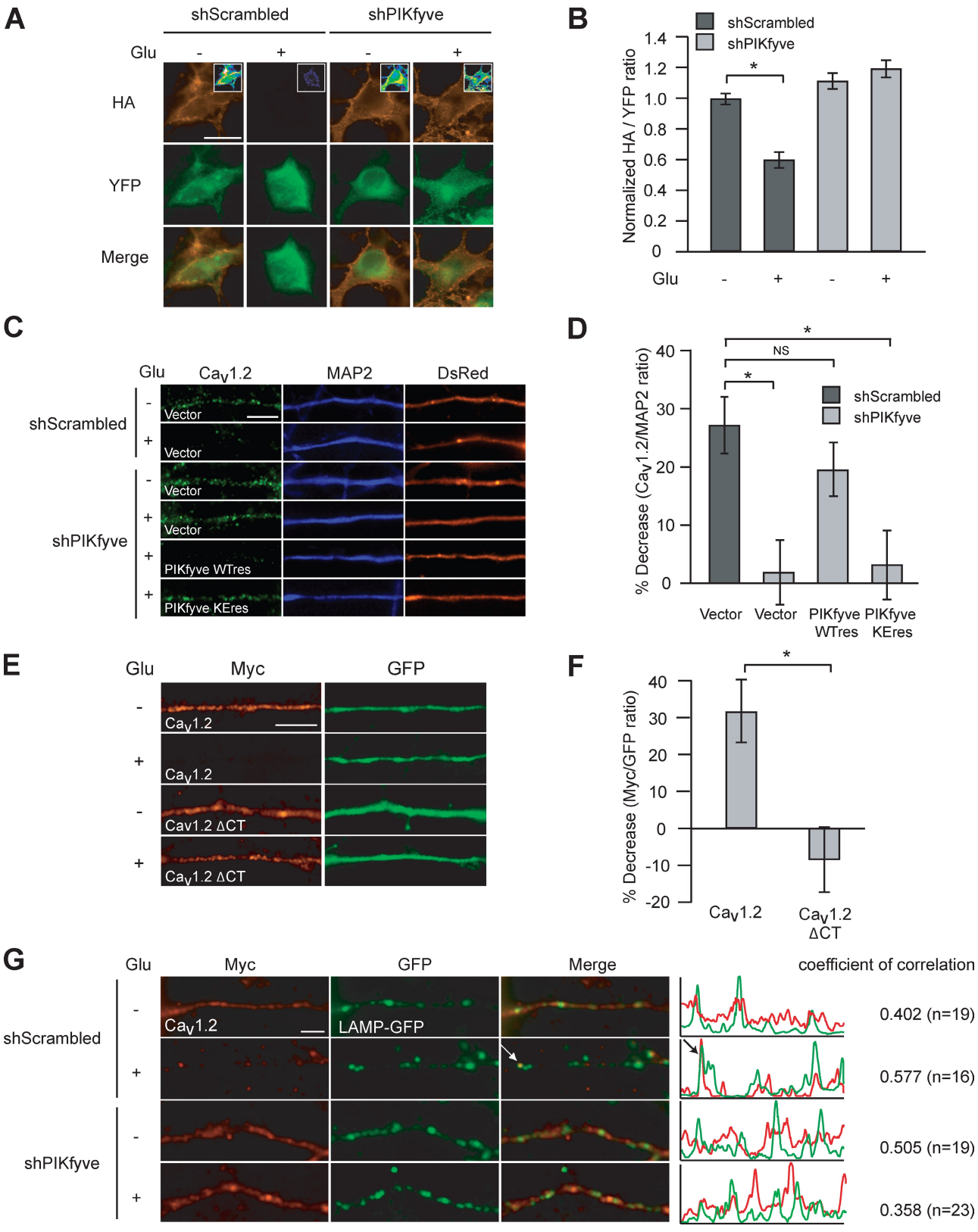

Figure 6. **PIKfyve regulates glutamate-dependent $Ca_V1.2$ internalization and degradation.** (A) Cortical neurons expressing YFP-HA-$Ca_V1.2$ with shPIKfyve or shScrambled were treated with 50 µM glutamate (Glu) for 10 min and stained with anti-HA antibodies without membrane permeabilization. The insets show the same images using a rainbow scheme. (B) Graph of the data in A illustrating the cell surface expression levels of $Ca_V1.2$ (n = 30; mean ± SEM; *, P < 0.0001 by Student's t test). (C) Dendrites from neurons stained with anti-$Ca_V1.2$ and anti-MAP2 antibodies and expressing either shPIKfyve or shScrambled, along with either a control vector or PIKfyve WTres or PIKfyve KEres. Neurons were stimulated with 50 µM glutamate for 10 min and then stained with anti-$Ca_V1.2$ or MAP2 antibodies. (D) Percent decrease of the ratio of $Ca_V1.2$ to MAP2 fluorescence on dendrites for the experiments in C (n = 100 dendrites; mean ± SEM; *, P < 0.01 by one-way ANOVA). (E) Dendrites from neurons expressing Flag-Myc-$Ca_V1.2$ or Flag-Myc–$Ca_V1.2$ ΔCT

The observation that Ca^{2+} influx through LTCs can contribute to toxicity led us to ask whether one of the functions of PIKfyve-dependent $Ca_V1.2$ degradation might be to reduce Ca^{2+}-dependent toxicity in neurons. To answer this question, we transfected neurons with either shScrambled or shPIKfyve and treated the cells with 50 µM glutamate for 10 min. 50 µM glutamate for 10 min did not cause cell death in untransfected neurons or neurons containing shScrambled (Fig. 7 C and Fig. S1). In contrast, treatment with glutamate caused a large increase in apoptosis in shPIKfyve-containing neurons (Fig. 7, C and D). The increase in glutamate-induced cell death in cells containing shPIKfyve was prevented by expression of PIKfyve WTres but not by PIKfyve KEres, indicating that the effects of shPIKfyve are specific and that the kinase activity of PIKfyve is required for its effect on survival. Together, these results strongly suggest that PIKfyve is important for protecting neurons from apoptosis under conditions of moderate glutamate receptor activation.

To determine whether PIKfyve protects neurons from excitotoxicity by mediating internalization and degradation of $Ca_V1.2$ channels, we transfected neurons with shPIKfyve and treated them with 50 µM glutamate for 10 min in the presence or absence of the $Ca_V1.2$ blocker nimodipine. We found that blocking $Ca_V1.2$ channels protected ~30% of the neurons lacking PIKfyve from glutamate-induced toxicity (Fig. 7 E), suggesting that excess Ca^{2+} entry through LTCs contributes to the increased sensitivity to glutamate in the absence of PIKfyve. Because AMPA receptors also contribute to excitotoxic cell death and these receptors are also known to be internalized in response to treatment of cells with glutamate, we investigated whether blocking AMPA receptors alone or in combination with LTCs prevented glutamate-induced cell death in neurons lacking PIKfyve. Blocking AMPA receptors expressing the shPIKfvye shRNA reduced cell death by ~30%, whereas the combination of both LTC and AMPA blockers almost completely prevented cell death in neurons. This result argues that the susceptibility to glutamate-induced apoptosis in neurons lacking PIKfyve is caused by the activity of both LTCs and AMPA receptors (Fig. 7 F).

This result also raised the interesting possibility that AMPA receptor internalization in response to glutamate might be mediated by PIKfyve. We examined this hypothesis by introducing into neurons one of the subunits of the AMPA receptor, the GluR2 channel, tagged with an intracellular YFP and an extracellular HA tag. This construct was robustly internalized by treatment of neurons with 50 µM glutamate for 10 min. However, introduction of the PIKfyve shRNA completely prevented GluR2 internalization, indicating that this event also depends on PIKfyve (Fig. S5, C–E). In control experiments, we also tested the role of PIKfyve in regulating the internalization of $K_V1.2$ channels but found that the surface expression of these channels did not depend on PIKfyve (Fig. S5, F and G). Thus, PIKfyve seems to be important for the internalization of at least one other channel in addition to $Ca_V1.2$ but not for all cell surface channels.

Discussion

This study provides new insights into the mechanisms by which neurons are protected from excessive Ca^{2+} influx and excitotoxicity after excessive activation of NMDA receptors, such as what occurs during transient ischemic attacks, epileptic seizures, and in the penumbra of strokes. Our results suggest that neurons internalize $Ca_V1.2$ channels and AMPA receptors in response to sustained activation of glutamate receptors. This is followed by recruitment of PIKfyve to the early endosomes, probably by binding to the C terminus of $Ca_V1.2$ and to lipids that are enriched in the endosomal membrane. Recruitment of PIKfyve to the endosomes leads to an increase in PtdIns(3,5)P_2 levels in these vesicles, which promotes their maturation and eventual fusion with lysosomes and leads to $Ca_V1.2$ degradation (Fig. 8). Thus, prolonged activation of NMDA receptors leads to both removal and degradation of $Ca_V1.2$ channels by a PIKfyve-dependent mechanism.

This PIKfyve-mediated degradation pathway seems to be essential for the ability of neurons to respond to moderate elevations of extracellular glutamate. Reducing PIKfyve or disrupting PIKfyve's association with $Ca_V1.2$ channels prevents channel degradation and leads to cell death when neurons are stimulated with subtoxic concentrations of glutamate. Blocking LTCs and AMPA receptors blocks the increase in cell death in neurons lacking PIKfyve, indicating that these ion channels can be toxic even at moderate levels of excitability and need to be down-regulated. The increased susceptibility of neurons to excitotoxicity in the absence of PIKfyve may help to explain why diseases that arise from mutations that alter PtdIns(3,5)P_2 levels disproportionately affect excitable cells such as neurons.

PtdIns(3,5)P_2 and membrane protein degradation in neurons

The important finding is that intracellular Ca^{2+} elevations in mammalian neurons regulate the levels of PtdIns(3,5)P_2. Circumstantial evidence suggests that Fab1 function may be regulated by Ca^{2+} signals in other organisms as well. In budding yeast, PtdIns(3,5)P_2 levels are increased by hyperosmotic shock, a process which increases the concentration of intracellular Ca^{2+}. In addition, Fab1 mutants are hypersensitive to elevated extracellular Ca^{2+} levels, suggesting that this pathway is important for the response to Ca^{2+}-induced stress. Finally, in fission yeast, mutations of *sst1*, a vesicular Ca^{2+} transporter, suppress the phenotype of cells containing mutations of the Fab1 homologue *ste12* (Matsumoto et al., 2002; Onishi et al., 2003). Our data and these corroborating studies suggest that Ca^{2+} regulation of PIKfyve activity might be a relatively ancient mechanism for cellular

together with GFP, stimulated with glutamate, and immunostained with anti-Myc and anti-GFP antibodies. (F) The graph shows the percent decrease in the ratio of $Ca_V1.2$ to MAP2 fluorescence in dendrites in E (n = 100 dendrites; mean ± SEM; *, $P < 0.005$ by Student's t test). (G) Dendrites from neurons expressing Flag-Myc-$Ca_V1.2$ and LAMP-GFP in the presence or absence of shPIKfyve or shScrambled. Cells were stained with anti-Myc and anti-GFP antibodies before and after treatment with 50 µM glutamate for 15 min. (n = 5 neurons and 16–23 dendrites). The arrow shows $Ca_V1.2$ colocalization with the lysosomal marker LAMP-GFP. Bars: (A) 10 µm; (C, E, and G) 5 µm.

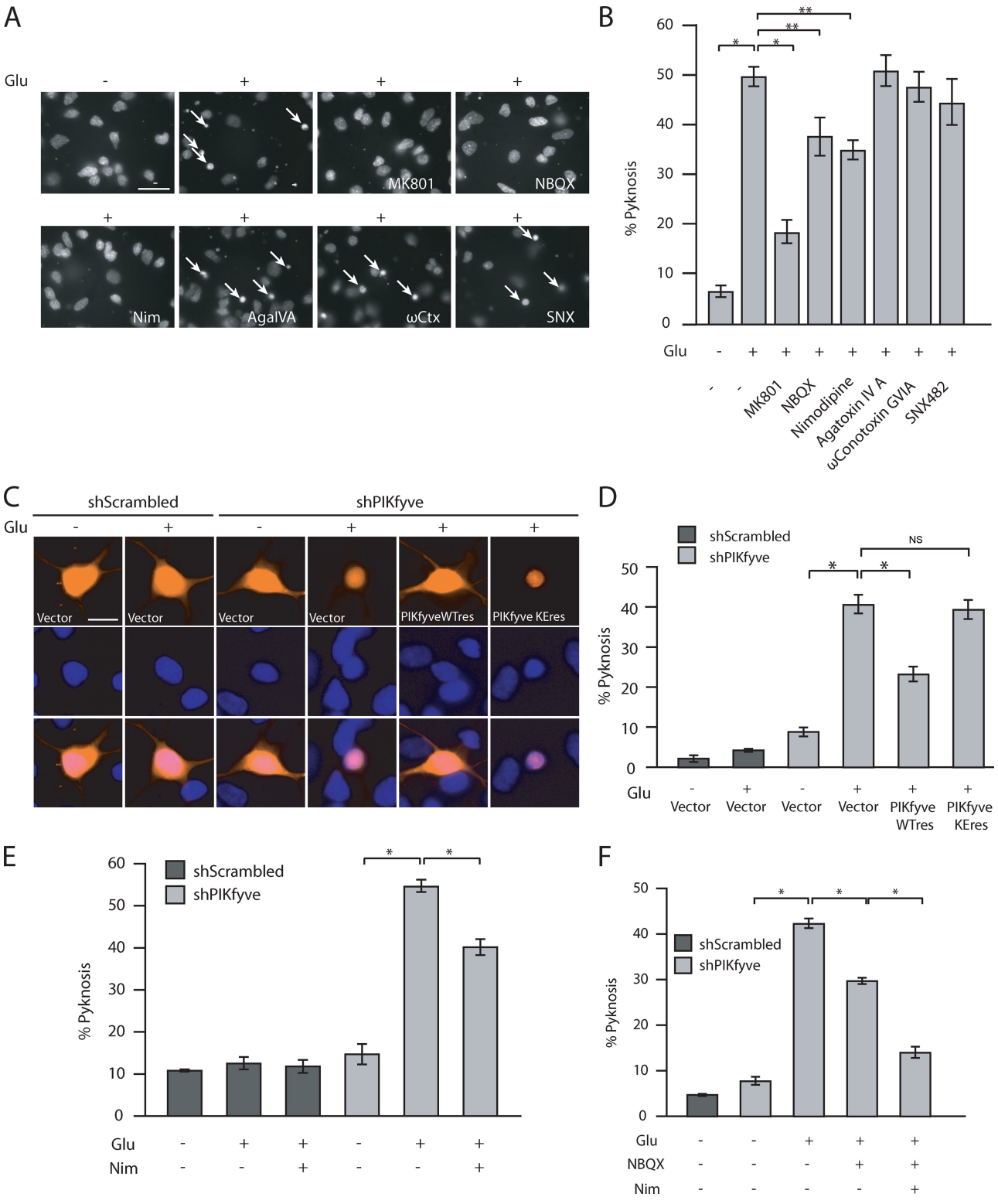

Figure 7. **PIKfyve protects neurons against excitotoxic cell death.** (A) Cortical neurons incubated with or without 10 µM MK801, 10 µM NBQX, 10 µM nimodipine (Nim), 0.5 µM agatoxin IVA (AgaIVA), 1 µM ω-conotoxin GVIA (ωCtx), or 10 µM SNX482 (SNX) and stimulated with 50 µM glutamate (Glu) for 30 min and then incubated for 9.5 h before analysis. Arrows indicate typical pyknotic cells. (B) Pyknotic nuclei quantified for each condition in A (n = 3 and >500 cells/sample; mean ± SEM; *, $P < 0.001$; and **, $P < 0.05$ by one-way ANOVA). (C) Cortical neurons were stimulated with 50 µM glutamate for 10 min and then incubated for 10 h in the absence of glutamate. Representative images of neurons expressing DsRed and either shPIKfyve or shScrambled along with the PIKfyve WTres, PIKfyve KEres, or the corresponding empty vector are shown. Cells were stained with the nuclear dye Hoechst. (D) Cell death was measured by counting pyknotic nuclei (n = 3 and >50 cells/sample; mean ± SEM; *, $P < 0.001$ by one-way ANOVA). (E) Cortical neurons were stimulated with 50 µM glutamate for 10 min in the presence or absence of 10 µM nimodipine and then incubated for 10 h. Cell death was measured by counting pyknotic nuclei (n = 3 and >50 cells/sample; mean ± SEM; *, $P < 0.001$ by one-way ANOVA). (F) Cortical neurons treated as in E. When indicated, NBQX was added at a 10-µM concentration (mean ± SEM; *, $P < 0.001$ by one-way ANOVA). Bars: (A) 30 µm; (C) 10 µm.

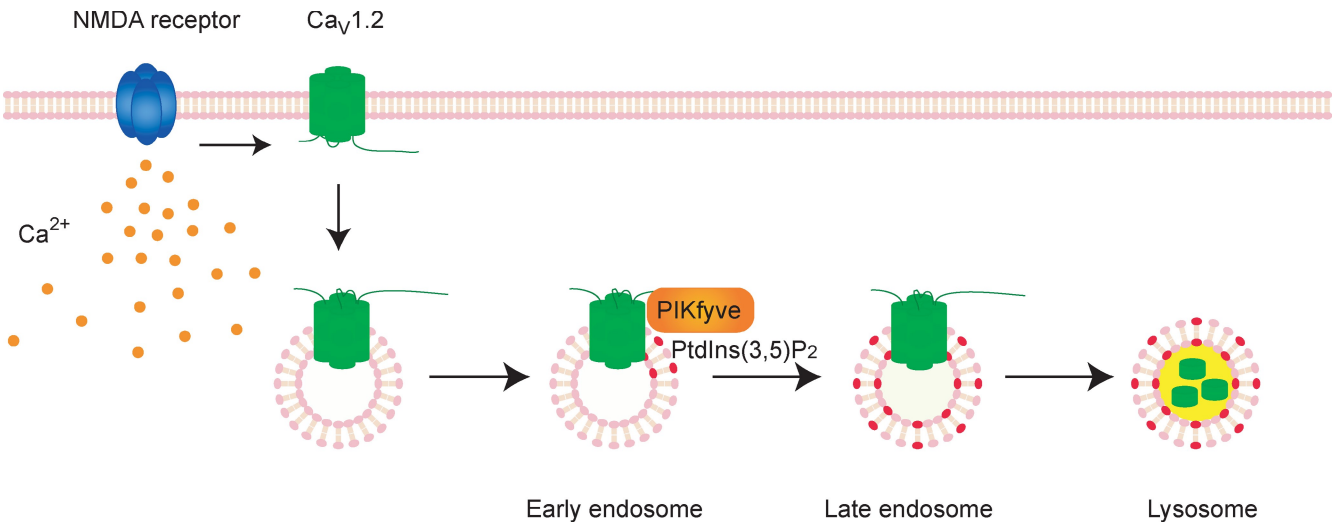

Figure 8. **Model describing the process of $Ca_V1.2$ degradation in response to glutamate.** Glutamate stimulation and high levels of intracellular Ca^{2+} lead to channel degradation in a PIKfyve-dependent manner, which protects the cell from Ca^{2+} toxicity. Stronger stimulation overrides this protective mechanism, and neurons undergo excitotoxicity.

protection, although this hypothesis clearly needs to be investigated further in other systems.

Because PIKfyve seems to play a general role in the degradation of a variety of cell surface proteins, it is interesting to speculate why it interacts with $Ca_V1.2$ channels. One possibility is that endosomes derived from Ca^{2+}-dependent endocytosis in dendrites and synapses often contain $Ca_V1.2$ channels. By binding to $Ca_V1.2$, PIKfyve can be recruited to a specific type of activity-dependent endosome and can play a role in the degradation of postsynaptic proteins. This is consistent with the general notion that the recruitment of proteins that contain FYVE domains to endosomal membranes is mediated by binding to both PtdIns(3)P and proteins located on endosomes (Simonsen et al., 1998; Lawe et al., 2000). It will be interesting to determine whether PIKfyve also participates in the Ca^{2+}-dependent degradation of other postsynaptic proteins such as NMDA receptors and whether this depends on PIKfyve binding to $Ca_V1.2$ channels.

Although PIKfyve has been reported to play a role in endosomal trafficking and lysosome function, it has not been shown to control endocytosis directly. We found that PIKfyve knockdown prevents $Ca_V1.2$ and AMPA receptor internalization in response to glutamate. This finding suggests either that PIKfyve can regulate the endocytic machinery directly or, alternatively, that altering endosome trafficking can prevent the activity or recycling of molecules required for endocytosis. The fact that we only observe PIKfyve in endosomes and not at the cell membrane argues that the effects of PIKfyve on endocytosis are indirect, but this question will need to be studied more carefully in the future.

PtdIns(3,5)P_2 and disease

Our finding that PIKfyve interacts with $Ca_V1.2$ and regulates its degradation also has important implications for the pathology of several diseases that affect myocytes and neurons. These cells express large numbers of $Ca_V1.2$ channels, suggesting that some aspects of the pathology observed in these patients could be caused by dysregulation of VGCCs or, more generally, by failure of activity-dependent protein degradation. If this hypothesis is correct, patients with PtdIns(3,5)P_2 phosphatase mutations might benefit from the use of Ca^{2+} channel blockers like gabapentin and pregabalin, which are widely used clinically for other applications.

In summary, our study identifies a novel mechanism for Ca^{2+} channel degradation in neurons that integrates two unrelated fields, Ca^{2+} channel signaling and endosomal trafficking. These experiments provide new insights into channel homeostasis and suggest a rationale for investigating Ca^{2+} channel dysfunction in diseases caused by defects in PtdIns(3,5)P_2 signaling.

Materials and methods

Materials and antibodies

Lipofectamine 2000, terminal deoxynucleotidyl transferase, Fura-2 acetoxymethyl ester, and Hoechst 33258 were purchased from Invitrogen; MK801, NBQX, and nimodipine were purchased from Sigma-Aldrich; SNX482 was purchased from Alomone Labs; DL-AP3 was purchased from Tocris Bioscience; bafilomycin A1 and lactacystin were purchased from EMD; chloroquine was purchased from MP Biomedicals; biotin–deoxy-UTP was purchased from TriLink BioTechnologies; and fluorescein-conjugated streptavidin (DTAF-streptavidin) was purchased from Jackson ImmunoResearch Laboratories, Inc. Antibodies to $Ca_V1.2$ (1:500; AB5156; Millipore), PIKfyve (1:500; 6C7; Abnova), Myc (1:500; 4A6; Millipore), HA (3F10; Roche), Flag (1:500; M2; Sigma-Aldrich), GAPDH (1:1,000; 6C5; Applied Biosystems), or DsRed (1:500; E64-1077; BD) was used for immunoblot analysis. Antibodies to $Ca_V1.2$ (1:100; AB5156), MAP2 (1:500; MAB378; Millipore), Myc (1:500; 4A6), HA (1:500; 3F10), PtdIns(3,5)P_2 (1:100; Z-P035; Echelon), or GFP (1:500; 598; MBL) was used for immunocytochemistry.

Cell culture, stimulation, and transfection

HEK 293T and NIH3T3 cells were cultured in Dulbecco's modified minimum essential medium containing 10% FBS, 100 U penicillin and 100 µg streptomycin (P/S), and 2 mM L-glutamine (Q). Neuro2A cells were cultured in minimum essential medium containing 10% FBS and P/S. Primary neuronal cultures were prepared from embryonic day 17–19 Sprague-Dawley rats by dissociating dissected cortices with enzyme solution (Hanks' balanced salt solution with 600 U papain and 0.32 mg/ml cystein). Neurons were plated on coverslips coated with 20 µg/ml polyornithine and 1.42 µg/ml laminin and maintained in culture in Basal Medium Eagle with

5% FBS, P/S, Q, and 0.6% glucose. For immunocytochemistry, neurons were stimulated with glutamate in Tyrode's solution without Mg (129 mM NaCl, 5 mM KCl, 3 mM $CaCl_2$, 30 mM glucose, 0.1% BSA, and 25 mM Hepes, pH 7.4). Cell lines and cortical neurons were transfected with plasmids using Lipofectamine 2000 according to the manufacturer's instructions. The ratio of plasmids used for specific experiments is given as follows: for surface expression assay, α1C/β1b/α2δ = 2:1:1 (Fig. 1, A–C) and α1C/β1b/α2δ/shRNA = 2:1:1:2 (Fig. 6, A and B); for colocalization assay, α1C/β1b/α2δ/LAMP = 2:1:1:1 (Fig. 3 C) and α1C/β1b/α2δ/LAMP/shRNA = 2:1:1:1:1 (Fig. 6 G); for coimmunoprecipitation, PIKfyve/Ca_V1.2 CT = 1:1 (Fig. 4, A and B), PIKfyve/α1C/β1b = 2:2:1 (Fig. 4 C), PIKfyveΔ/Ca_V1.2 CT = 1:1 (Fig. 4, E and F), and PIKfyve/Ca_V1.2 ΔCT = 1:1 (Fig. 4 H); for relocalization of the GRAM domain, GRAM/shRNA/PIKfyve = 1:2:2 (Fig. 5 F); for Ca_V1.2 degradation assay, PIKfyve/shRNA = 1:1 (Fig. 6, C and D) and α1C/β1b/α2δ = 2:1:1 (Fig. 6, E and F); and for cell death assay, shRNA/PIKfyve = 1:1 (Fig. 7, C and D).

Plasmid construction

GFP-PIKfyve (mouse) and GFP-HA-K_V1.2 constructs were provided by P. Cullen (University of Bristol, Bristol, England, UK; Rutherford et al., 2006) and L.Y. Jan (University of California, San Francisco, San Francisco, CA; Gu et al., 2003), respectively. The cDNA for PIKfyve was amplified by PCR from the GFP-PIKfyve construct and cloned into the XbaI sites of pCS4-Myc and pCS4-HA. The pCS4-GFP, pCS4-Cherry, and pCS4-HA-GFP plasmids were constructed by the insertion of the EGFP and Cherry coding sequence into the XbaI site in pCS4 and pCS4-HA, respectively. The Rab5, LAMP1, and MTM1 cDNAs were amplified by PCR from the human ORFeome cDNA library (Thermo Fisher Scientific) and subcloned into the BamHI sites of pcDNA3-GFP, pCS4-GFP, pCS4-Cherry, and pCS4-Myc to generate three different vectors encoding each protein. The GluR2 cDNA was amplified from the human ORFeome cDNA library and subcloned into the XbaI sites of pCS4-HA-GFP. The dihydropyridine-resistant Ca_V1.2 α1C, β1b, α2δ, and pEYFP-HA-Ca_V1.2 constructs were described previously (Dolmetsch et al., 2001; Gomez-Ospina et al., 2006; Green et al., 2007). The pGW1-Flag-Ca_V1.2, pGW-Flag-α2δ, GST–Ca_V1.2 CT, and pDEST27-GST-YFP were generated using Gateway technology (Invitrogen). The cDNA for Ca_V1.2 CT was amplified by PCR and cloned into the BamHI site of pcDNA3-Flag. Short hairpin oligonucleotides were designed and inserted into the RNAi-Ready pSIREN-DNR-DsRed-Express vector (Takara Bio Inc.) by ligation into the BamHI and EcoRI sites. For specific experiments, DsRed was eliminated from the RNAi-Ready pSIREN-DNR-DsRed-Express vector using the NcoI restriction enzyme. Site-directed mutagenesis was performed using QuikChange (Agilent Technologies) to generate RNAi-resistant kinase-negative PIKfyve (PIKfyve KEres; Sbrissa et al., 2000). PIKfyve KEres consisted of changing the K^{1820} to E in the kinase domain. The cDNA from the GRAM domain of myotubularin (residues 8–112) was amplified by PCR from the MTM1 construct and cloned into pcDNA3-GFP.

The primers used were as follows: PIKfyve forward, 5′-ATCTAGAATGGCCACAGATGACAAG-3′; and reverse, 5′-GTCTAGATCAGCAATTCAGATCCAA-3′; PIKfyve FYVE forward, 5′-AGGATCCATGGCCACAGATGACAAG-3′; and reverse, 5′-GGGATCCCTAACTTAAGGCTATTTT-3′; PIKfyve DEP forward, 5′-GGGATCCTATGCTCATTCTACAGAC-3′; and reverse, 5′-AGGATCCTTATGAGAGCTGCTGTCC-3′; PIKfyve Cpn/TCP-1 forward, 5′-GAGATCTATAAGTGATGCCTTCATC-3′; and reverse, 5′-AAGATCTTTATGAGCATCTCATCCC-3′; PIKfyve linker forward, 5′-GAGATCTACTCGAGATTATTTTCCA-3′; and reverse, 5′-AAGATCTTTAGATGAATTCCTCCTC-3′; PIKfyve PIP5K forward, 5′-AGGATCCCGTTCCCTTTCTCACTCA-3′; and reverse, 5′-GGGATCCTCAGCAATTCAGATCCAA-3′; PIKfyve KEres sense, 5′-AGATTCATTCTGGAGCAAATGCCTCGTTTG-3′; and antisense, 5′-CAAACGAGGCATTTGCTCCAGAATGAATCT-3′; Ca_V1.2 CT-1 forward, 5′-GCCACCATGGTCGGCAAGCCCTCGCAGAGG-3′; and reverse, 5′-CTAGTTGCCAAACAGGCCTCCAGCCCTCCTG-3′; Ca_V1.2 CT-2 forward, 5′-GCCACCATGCACGTCAGCTACTACCAGAGTG-3′; and reverse, 5′-CTACTGTACCCGGACAGCAGGGGACAAGGG-3′; Ca_V1.2 CT-3 forward, 5′-GCCACCATGGAGGCAGCATGGAAACTCAGC-3′; and reverse, 5′-CTACTTTAGACATTCCAGATGGAAGGAGGC-3′; Ca_V1.2 CT-4 forward, 5′-GCCACCATGCGACAAAAGGATCAAGGGGGAG-3′; and reverse, 5′-CTAGCCCCCACTACAGGCTGTGGTCTCCTC-3′; Ca_V1.2 CT-5 forward, 5′-GCCACCATGAGCAGCATGGCCCGGAGAGCC-3′; and reverse, 5′-CTACAGGTTGCTGACATAGGACCTG-3′; GFP forward, 5′-AATCTAGAATGGTGAGCAAGGGCGAG-3′; and reverse, 5′-GGACTAGTTTACTTGTACAGCTCGTC-3′; Cherry forward, 5′-CTCTAGAGCCACCATGGTGAGCAAGGGCGAG-3′; and reverse, 5′-GACTAGTTTACTTGTACAGCTCGTCCATGCCGCC-3′; Rab5 forward, 5′-AGGATCCATGGCTAGTCGAGGCGC-3′; and reverse, 5′-GGGATCCTTAGTTACTACAACACTGATTCCTGG-3′; LAMP1 forward, 5′-AGGATCCGCCACCATGGCGGCCCCCGGCAG-3′; and reverse, 5′-GGGATCCGATAGTCTGGTAGCCTGCGTGACTCC-3′; MTM1 forward, 5′-AGGATCCGCCACCATGGCTTCTGCATCAACTTC-3′; and reverse, 5′-AGGATCCTCAGAAGTGAGTTTGCACATGGGG-3′; 2× GRAM forward, 5′-GGGATCCGCCACCATGAAATATAATTCACACTCC-3′; and reverse, 5′-AGAATTCAGTAATATCTAGACCATAGGAATT-3′; 2× GRAM forward, 5′-AGAATTCATGAAATATAATTCACACTCCTTG-3′; and reverse, 5′-AGGATCCAGTAATATCTAGACCATAGGAATTTTCTCC-3′; and GluR2 forward, 5′-GTCTAGAGCCACCATGCAAAAGATTATGCATAT-3′; and reverse, 5′-GTCTAGAAATTTTAACACTTTCGATGCCATA-3′.

The oligonucleotides used were as follows: mouse PIKfyve shRNA sense, 5′-GATCCGGACAGGGTTGGATCTGAATTCAAGAGATTCAGATCCAACCCTGTCCTTTTTTACGCGTG-3′; and antisense, 5′-AATTCACGCGTAAAAAAGGACAGGGTTGGATCTGAATCTCTTGAATTCAGATCCAACCCTGTCCG-3′; rat PIKfyve shRNA sense, 5′-GATCCGGACAGGGTTGGATCTCAATTCAAGAGATTGAGATCCAACCCTGTCCTTTTTTACGCGTG-3′; and antisense, 5′-AATTCACGCGTAAAAAAGGACAGGGTTGGATCTCAATCTCTTGAATTGAGATCCAACCCTGTCCG-3′; and shScrambled shRNA sense, 5′-GATCCTGTAGGTCGAGAGCGTAGATTCAAGAGATCTACGCTCTCGACCTACATTTTTTACGCGTG-3′; and antisense, 5′-AATTCACGCGTAAAAAATGTAGGTCGAGAGCGTAGATCTCTTGAATCTACGCTCTCGACCTACAG-3′. RNAi-resistant PIKfyve cDNA was made by introducing silent mutations using conventional PCR. The PCR primers used were as follows: forward, 5′-TCTAGAATGGCCACAGATGACAAGAGTTCCCCGACACTGGACTCTGCTAATGATTTG-3′; and reverse, 5′-TCTAGATTAGCAATTTAAGTCTAGTCCCGTCCAGTGGTCTGGCACCATCAAGAAATACTT-3′.

Immunocytochemistry

Cortical neurons plated on 12- or 15-mm coverslips and grown in 12- or 24-well plates were fixed with 4% paraformaldehyde in PBS for 10 min at room temperature. The coverslips were washed in PBS once and incubated with a blocking solution (5% BSA in PBS) with (for regular immunocytochemistry) or without (for surface expression assay) 0.4% Triton X-100 for 30 min. The samples were incubated with the indicated primary antibodies for 1 h at room temperature or overnight at 4°C and then washed three times in PBS at room temperature before incubation with secondary antibodies (Alexa Fluor 350 anti–mouse IgG [1:1,000], Alexa Fluor 488 anti–mouse/rabbit IgG [1:1,000], and/or Alexa Fluor 594 anti–mouse/rabbit IgG [1:1,000]) for 30 min at room temperature in the blocking solution. For surface expression assays, the samples were incubated with anti-HA antibodies (3F10) for 1 h at room temperature or overnight at 4°C and then incubated with secondary antibodies (Alexa Fluor 594 anti–rat IgG [1:1000]) for 30 min at room temperature in the blocking solution. Cells were imaged using an epifluorescence microscope (TE2000U; Nikon) equipped with 10× S Fluor 0.5 NA (Nikon), 40× S Fluor 1.30 NA (Nikon), and 60× Plan-Apochromat 1.40 NA (Nikon) objective lenses and a cooled charge-coupled device camera (ORCA-ER; Hamamatsu Photonics) controlled by a computer (Macintosh; Apple) running Open Laboratory software (PerkinElmer).

Image analysis

To measure the surface expression levels, the single regions were defined to encompass the entire cell body and calculate the ratio of HA to YFP fluorescence. To measure the relocalization of the GFP–2× GRAM in neurons, fluorescent images were obtained and analyzed using Open Laboratory software. For each cell, five circular regions of interest (ROIs) were defined around the periphery of the cell nucleus, and a single ROI was defined to encompass the entire cell body. The mean fluorescence intensity calculated from the ROIs around the nucleus was divided by the mean intensity of the entire cell body to generate a perinuclear ratio value (P). The percent change in P in stimulated cells was calculated using the following equation: $\%P = (P_S - P_R)/P_R$, where P_S is the ratio after stimulation and P_R is the ratio in resting cells. Stimulation of cells with glutamate resulted in an increase in puncta that could be detected using the anti-PtdIns(3,5)P_2 antibodies. To quantify the number of puncta, the raw fluorescence images were intensity sliced to generate binary images that included only pixels that were part of a puncta. The area covered by the puncta was divided by the total area of the cell to generate a value for the percentage of pixels in a cell that formed part of a puncta. Colocalization of Flag-Myc-Ca_V1.2 and LAMP-GFP was evaluated by using line profiles drawn along neuronal dendrites for each type of staining using Igor Pro software (WaveMetrics). The coefficient of correlation between the Flag-Myc-Ca_V1.2 and LAMP-GFP line profiles was calculated according to the following equation:

$$Correlation(x,y) = \frac{\sum (x-\bar{x})(y-\bar{y})}{\sqrt{\sum (x-\bar{x})^2 \sum (y-\bar{y})^2}}.$$

Immunoblot analysis

Cells were washed with PBS and then lysed in extraction buffer (20 mM Tris-HCl, pH 7.5, 150 mM NaCl, 5 mM EGTA, 5 µM NaF, 1 µM Na_3VO_4, 0.5% Triton X-100, and 1 mM dithiothreitol) containing a protease inhibitor cocktail tablet (Roche). The cell lysates were analyzed by SDS-PAGE, transferred to polyvinylidene fluoride, probed with primary antibodies, and detected with HRP-conjugated secondary antibodies and luminol reagent (SuperSignal West Dura Extended Duration Substrate; Thermo Fisher Scientific).

Coimmunoprecipitation

Transfected HEK 293T cells were washed with PBS and then lysed in extraction buffer containing protease inhibitors (see Immunoblot analysis). The cell lysates were centrifuged at 13,200 rpm for 10 min, and the resulting supernatant was subjected to immunoprecipitation with antibodies to 10 µg/ml PIKfyve (6C7), 2.5 µg/ml Myc (4A6), or anti-Flag M2 agarose beads (Sigma-Aldrich) for 3 h at 4°C. The immunoprecipitates were subjected to immunoblot analysis with antibodies to $Ca_V1.2$, Myc, Flag, and HA.

Proteomics and mass spectrometry

The protein complex associated with the C terminus of $Ca_V1.2$ was purified and analyzed using mass spectrometry three independent times. One immunoprecipitated sample was analyzed in duplicate to generate a total of five mass spectrometry data samples. For each experiment, three 10-cm plates of Neuro2A cells were transfected with GST-YFP or with GST–$Ca_V1.2$ CT using Lipofectamine 2000 according to the manufacturer's instructions (24 µg DNA/plate in 1.5 ml of Opti-MEM-I and 60 µl of Lipofectamine in 1.5 ml of Opti-MEM-I). 2 d after transfection, the cells were lysed in lysis buffer (50 mM Tris-HCl, 1% Triton X-100, 150 mM NaCl, and 10 mM EDTA) for 30 min at 4°C with shaking. The lysis buffer was supplemented with an inhibitor cocktail tablet (Roche) and calpain I and II inhibitors. The lysates were centrifuged for 20 min at 14,000 rpm and incubated with 100 µl of glutathione Sepharose beads (GE Healthcare) for 2 h at 4°C. The beads were washed five times in lysis buffer and treated with trypsin before analysis. The peptides were separated using capillary electrophoresis and analyzed by tandem mass spectrometry in the Stanford University Mass Spectrometry facility. Finally, all of the peptide sequences were analyzed using MASCOT software (Matrix Science).

Ca^{2+} imaging

Cortical neurons were loaded with 1 µM Fura-2 for 30 min at 37°C in Tyrode's solution (129 mM NaCl, 5 mM KCl, 2 mM $CaCl_2$, 1 mM $MgCl_2$, 30 mM glucose, 0.1% BSA, and 25 mM Hepes, pH 7.4), washed with Tyrode's solution, and placed in a perfusion chamber on the stage of an inverted fluorescence microscope (TE2000U; Nikon). The cells were treated with 50 µM glutamate in Tyrode's solution without Mg (129 mM NaCl, 5 mM KCl, 3 mM $CaCl_2$, 30 mM glucose, 0.1% BSA, and 25 mM Hepe, pH 7.4) for 10 min before imaging in normal Tyrode's solution and then stimulated with high KCl Tyrode's solution (67 mM NaCl, 67 mM KCl, 2 mM $CaCl_2$, 1 mM $MgCl_2$, 30 mM glucose, 0.1% BSA, and 25 mM Hepes, pH 7.4). Imaging was performed at room temperature on an epifluorescence microscope (Eclipse TE2000U; Nikon) equipped with an excitation wheel and an automated stage. Open Laboratory software was used to collect and quantify time-lapse excitation ratio images. Fluorescence images were analyzed using Igor Pro software.

Cell death assay

Cortical neurons were stimulated with 50 µM glutamate for the indicated times and were then incubated for 10 h in the absence of glutamate. Neurons were then fixed with 4% paraformaldehyde in PBS for 10 min at room temperature. The coverslips were incubated in a solution (10 µM Hoechst 33258 and 0.4% Triton X-100 in PBS) for 10 min to stain the nuclei. Fluorescence images were obtained by epifluorescence microscopy, and pyknotic nuclei were counted. For TUNEL assay, neurons were fixed with 4% paraformaldehyde in PBS for 15 min at room temperature and incubated with 0.1% Triton X-100 in PBS for 10 min. The samples were then incubated with TUNEL reaction solution (15 U terminal deoxynucleotidyl transferase, 40 µM biotin–deoxy-UTP, 0.1 M potassium cacodylate, 2 mM $CoCl_2$, and 0.2 mM DTT) for 1 h at 37°C and washed three times in PBS at room temperature before incubation with DTAF-streptavidin (1:800) for 45 min at 37°C. The samples were then incubated in a solution (10 µM Hoechst 33258 in PBS) for 10 min to stain the nuclei.

Online supplemental material

Fig. S1 shows that glutamate stimulation promotes neuronal cell death. Fig. S2 shows that glutamate stimulation promotes $Ca_V1.2$ relocalization and degradation. Fig. S3 shows localization of LAMP, PIKfyve, and the GRAM domain. Fig. S4 shows that knockdown of PIKfyve by PIKfyve shRNAs promotes vacuole formation. Fig. S5 shows that PIKfyve is important for specific channel internalization and degradation. Table S1 lists $Ca_V1.2$-interacting proteins. Online supplemental material is available at http://www.jcb.org/cgi/content/full/jcb.200903028/DC1.

We thank Drs. Petter Cullen and Lily Yeh Jan for the PIKfyve and $K_V1.2$ constructs and Drs. Deborah Solymar, Elizabeth Nigh, Ben Barres, and Thomas Clandinin for critical reading of the manuscript.

This work was supported by grants and awards from the National Institutes of Health (RO1 NS048564), McKnight Scholar, Searle Scholar (to R.E. Dolmetsch), American Heart Association, Japan Society for the Promotion of Science, Mochida Memorial Foundation for Medical and Pharmaceutical Research (to F. Tsuruta), National Institutes of Health Medical Scientist Training Program (to E.M. Green), and Foundation Philippe (to M. Rousset).

Submitted: 6 March 2009
Accepted: 11 September 2009

References

Botelho, R.J., J.A. Efe, D. Teis, and S.D. Emr. 2008. Assembly of a Fab1 phosphoinositide kinase signaling complex requires the Fig4 phosphoinositide phosphatase. *Mol. Biol. Cell.* 19:4273–4286. doi:10.1091/mbc.E08-04-0405

Budde, T., S. Meuth, and H.C. Pape. 2002. Calcium-dependent inactivation of neuronal calcium channels. *Nat. Rev. Neurosci.* 3:873–883. doi:10.1038/nrn959

Calin-Jageman, I., and A. Lee. 2008. Ca(v)1 L-type Ca2+ channel signaling complexes in neurons. *J. Neurochem.* 105:573–583. doi:10.1111/j.1471-4159.2008.05286.x

Catterall, W.A. 2000. Structure and regulation of voltage-gated Ca2+ channels. *Annu. Rev. Cell Dev. Biol.* 16:521–555. doi:10.1146/annurev.cellbio.16.1.521

Chan, C.S., J.N. Guzman, E. Ilijic, J.N. Mercer, C. Rick, T. Tkatch, G.E. Meredith, and D.J. Surmeier. 2007. 'Rejuvenation' protects neurons in mouse models of Parkinson's disease. *Nature*. 447:1081–1086. doi:10.1038/nature05865

Chow, C.Y., Y. Zhang, J.J. Dowling, N. Jin, M. Adamska, K. Shiga, K. Szigeti, M.E. Shy, J. Li, X. Zhang, et al. 2007. Mutation of FIG4 causes neurodegeneration in the pale tremor mouse and patients with CMT4J. *Nature*. 448:68–72. doi:10.1038/nature05876

Coon, A.L., D.R. Wallace, C.F. Mactutus, and R.M. Booze. 1999. L-type calcium channels in the hippocampus and cerebellum of Alzheimer's disease brain tissue. *Neurobiol. Aging*. 20:597–603. doi:10.1016/S0197-4580(99)00068-8

Davis, S.F., and C.L. Linn. 2003. Activation of NMDA receptors linked to modulation of voltage-gated ion channels and functional implications. *Am. J. Physiol. Cell Physiol.* 284:C757–C768.

Day, M., Z. Wang, J. Ding, X. An, C.A. Ingham, A.F. Shering, D. Wokosin, E. Ilijic, Z. Sun, A.R. Sampson, et al. 2006. Selective elimination of glutamatergic synapses on striatopallidal neurons in Parkinson disease models. *Nat. Neurosci.* 9:251–259. doi:10.1038/nn1632

Derkach, V.A., M.C. Oh, E.S. Guire, and T.R. Soderling. 2007. Regulatory mechanisms of AMPA receptors in synaptic plasticity. *Nat. Rev. Neurosci.* 8:101–113. doi:10.1038/nrn2055

Disterhoft, J.F., J.R. Moyer Jr., and L.T. Thompson. 1994. The calcium rationale in aging and Alzheimer's disease. Evidence from an animal model of normal aging. *Ann. N. Y. Acad. Sci.* 747:382–406.

Dolmetsch, R.E., U. Pajvani, K. Fife, J.M. Spotts, and M.E. Greenberg. 2001. Signaling to the nucleus by an L-type calcium channel-calmodulin complex through the MAP kinase pathway. *Science*. 294:333–339. doi:10.1126/science.1063395

Dong, Z., P. Saikumar, J.M. Weinberg, and M.A. Venkatachalam. 2006. Calcium in cell injury and death. *Annu. Rev. Pathol.* 1:405–434. doi:10.1146/annurev.pathol.1.110304.100218

Duex, J.E., F. Tang, and L.S. Weisman. 2006. The Vac14p–Fig4p complex acts independently of Vac7p and couples $PI3,5P_2$ synthesis and turnover. *J. Cell Biol.* 172:693–704. doi:10.1083/jcb.200512105

Efe, J.A., R.J. Botelho, and S.D. Emr. 2005. The Fab1 phosphatidylinositol kinase pathway in the regulation of vacuole morphology. *Curr. Opin. Cell Biol.* 17:402–408. doi:10.1016/j.ceb.2005.06.002

Gary, J.D., A.E. Wurmser, C.J. Bonangelino, L.S. Weisman, and S.D. Emr. 1998. Fab1p is essential for PtdIns(3)P 5-kinase activity and the maintenance of vacuolar size and membrane homeostasis. *J. Cell Biol.* 143:65–79. doi:10.1083/jcb.143.1.65

Gomez-Ospina, N., F. Tsuruta, O. Barreto-Chang, L. Hu, and R. Dolmetsch. 2006. The C terminus of the L-type voltage-gated calcium channel Ca(V)1.2 encodes a transcription factor. *Cell*. 127:591–606. doi:10.1016/j.cell.2006.10.017

Green, E.M., C.F. Barrett, G. Bultynck, S.M. Shamah, and R.E. Dolmetsch. 2007. The tumor suppressor eIF3e mediates calcium-dependent internalization of the L-type calcium channel CaV1.2. *Neuron*. 55:615–632. doi:10.1016/j.neuron.2007.07.024

Gu, C., Y.N. Jan, and L.Y. Jan. 2003. A conserved domain in axonal targeting of Kv1 (Shaker) voltage-gated potassium channels. *Science*. 301:646–649. doi:10.1126/science.1086998

Haase, H., A. Kresse, A. Hohaus, H.D. Schulte, M. Maier, K.J. Osterziel, P.E. Lange, and I. Morano. 1996. Expression of calcium channel subunits in the normal and diseased human myocardium. *J. Mol. Med.* 74:99–104. doi:10.1007/BF00196785

Hell, J.W., R.E. Westenbroek, C. Warner, M.K. Ahlijanian, W. Prystay, M.M. Gilbert, T.P. Snutch, and W.A. Catterall. 1993. Identification and differential subcellular localization of the neuronal class C and class D L-type calcium channel alpha 1 subunits. *J. Cell Biol.* 123:949–962. doi:10.1083/jcb.123.4.949

Ikonomov, O.C., D. Sbrissa, and A. Shisheva. 2001. Mammalian cell morphology and endocytic membrane homeostasis require enzymatically active phosphoinositide 5-kinase PIKfyve. *J. Biol. Chem.* 276:26141–26147. doi:10.1074/jbc.M101722200

Jarvis, S.E., and G.W. Zamponi. 2007. Trafficking and regulation of neuronal voltage-gated calcium channels. *Curr. Opin. Cell Biol.* 19:474–482. doi:10.1016/j.ceb.2007.04.020

Korenkov, A.I., J. Pahnke, K. Frei, R. Warzok, H.W. Schroeder, R. Frick, L. Muljana, J. Piek, Y. Yonekawa, and M.R. Gaab. 2000. Treatment with nimodipine or mannitol reduces programmed cell death and infarct size following focal cerebral ischemia. *Neurosurg. Rev.* 23:145–150. doi:10.1007/PL00011946

Lau, C.G., and R.S. Zukin. 2007. NMDA receptor trafficking in synaptic plasticity and neuropsychiatric disorders. *Nat. Rev. Neurosci.* 8:413–426. doi:10.1038/nrn2153

Lawe, D.C., V. Patki, R. Heller-Harrison, D. Lambright, and S. Corvera. 2000. The FYVE domain of early endosome antigen 1 is required for both phosphatidylinositol 3-phosphate and Rab5 binding. Critical role of this dual interaction for endosomal localization. *J. Biol. Chem.* 275:3699–3705. doi:10.1074/jbc.275.5.3699

Matsumoto, T.K., A.J. Ellsmore, S.G. Cessna, P.S. Low, J.M. Pardo, R.A. Bressan, and P.M. Hasegawa. 2002. An osmotically induced cytosolic Ca2+ transient activates calcineurin signaling to mediate ion homeostasis and salt tolerance of *Saccharomyces cerevisiae*. *J. Biol. Chem.* 277:33075–33080. doi:10.1074/jbc.M205037200

Michell, R.H., V.L. Heath, M.A. Lemmon, and S.K. Dove. 2006. Phosphatidylinositol 3,5-bisphosphate: metabolism and cellular functions. *Trends Biochem. Sci.* 31:52–63. doi:10.1016/j.tibs.2005.11.013

Nicot, A.S., and J. Laporte. 2008. Endosomal phosphoinositides and human diseases. *Traffic*. 9:1240–1249. doi:10.1111/j.1600-0854.2008.00754.x

Nicot, A.S., H. Fares, B. Payrastre, A.D. Chisholm, M. Labouesse, and J. Laporte. 2006. The phosphoinositide kinase PIKfyve/Fab1p regulates terminal lysosome maturation in *Caenorhabditis elegans*. *Mol. Biol. Cell*. 17:3062–3074.

Odorizzi, G., M. Babst, and S.D. Emr. 1998. Fab1p PtdIns(3)P 5-kinase function essential for protein sorting in the multivesicular body. *Cell*. 95:847–858. doi:10.1016/S0092-8674(00)81707-9

Onishi, M., Y. Nakamura, T. Koga, K. Takegawa, and Y. Fukui. 2003. Isolation of suppressor mutants of phosphatidylinositol 3-phosphate 5-kinase deficient cells in *Schizosaccharomyces pombe*. *Biosci. Biotechnol. Biochem.* 67:1772–1779. doi:10.1271/bbb.67.1772

Orrenius, S., B. Zhivotovsky, and P. Nicotera. 2003. Regulation of cell death: the calcium-apoptosis link. *Nat. Rev. Mol. Cell Biol.* 4:552–565. doi:10.1038/nrm1150

Rusten, T.E., L.M. Rodahl, K. Pattni, C. Englund, C. Samakovlis, S. Dove, A. Brech, and H. Stenmark. 2006. Fab1 phosphatidylinositol 3-phosphate 5-kinase controls trafficking but not silencing of endocytosed receptors. *Mol. Biol. Cell*. 17:3989–4001. doi:10.1091/mbc.E06-03-0239

Rutherford, A.C., C. Traer, T. Wassmer, K. Pattni, M.V. Bujny, J.G. Carlton, H. Stenmark, and P.J. Cullen. 2006. The mammalian phosphatidylinositol 3-phosphate 5-kinase (PIKfyve) regulates endosome-to-TGN retrograde transport. *J. Cell Sci.* 119:3944–3957. doi:10.1242/jcs.03153

Sbrissa, D., O.C. Ikonomov, and A. Shisheva. 2000. PIKfyve lipid kinase is a protein kinase: downregulation of 5′-phosphoinositide product formation by autophosphorylation. *Biochemistry*. 39:15980–15989. doi:10.1021/bi001897f

Sbrissa, D., O.C. Ikonomov, Z. Fu, T. Ijuin, J. Gruenberg, T. Takenawa, and A. Shisheva. 2007. Core protein machinery for mammalian phosphatidylinositol 3,5-bisphosphate synthesis and turnover that regulates the progression of endosomal transport. Novel Sac phosphatase joins the ArPIKfyve-PIKfyve complex. *J. Biol. Chem.* 282:23878–23891. doi:10.1074/jbc.M611678200

Schurr, A. 2004. Neuroprotection against ischemic/hypoxic brain damage: blockers of ionotropic glutamate receptor and voltage sensitive calcium channels. *Curr. Drug Targets*. 5:603–618. doi:10.2174/1389450043345209

Simonsen, A., R. Lippé, S. Christoforidis, J.M. Gaullier, A. Brech, J. Callaghan, B.H. Toh, C. Murphy, M. Zerial, and H. Stenmark. 1998. EEA1 links PI(3)K function to Rab5 regulation of endosome fusion. *Nature*. 394:494–498. doi:10.1038/28879

Stotz, S.C., and G.W. Zamponi. 2001. Structural determinants of fast inactivation of high voltage-activated Ca(2+) channels. *Trends Neurosci.* 24:176–181. doi:10.1016/S0166-2236(00)01738-0

Thibault, O., and P.W. Landfield. 1996. Increase in single L-type calcium channels in hippocampal neurons during aging. *Science*. 272:1017–1020. doi:10.1126/science.272.5264.1017

Thibault, O., J.C. Gant, and P.W. Landfield. 2007. Expansion of the calcium hypothesis of brain aging and Alzheimer's disease: minding the store. *Aging Cell*. 6:307–317. doi:10.1111/j.1474-9726.2007.00295.x

Tsien, R.W., D. Lipscombe, D.V. Madison, K.R. Bley, and A.P. Fox. 1988. Multiple types of neuronal calcium channels and their selective modulation. *Trends Neurosci.* 11:431–438. doi:10.1016/0166-2236(88)90194-4

Tsujita, K., T. Itoh, T. Ijuin, A. Yamamoto, A. Shisheva, J. Laporte, and T. Takenawa. 2004. Myotubularin regulates the function of the late endosome through the gram domain-phosphatidylinositol 3,5-bisphosphate interaction. *J. Biol. Chem.* 279:13817–13824. doi:10.1074/jbc.M312294200

Westenbroek, R.E., M.K. Ahlijanian, and W.A. Catterall. 1990. Clustering of L-type Ca2+ channels at the base of major dendrites in hippocampal pyramidal neurons. *Nature*. 347:281–284. doi:10.1038/347281a0

Zhang, Y., S.N. Zolov, C.Y. Chow, S.G. Slutsky, S.C. Richardson, R.C. Piper, B. Yang, J.J. Nau, R.J. Westrick, S.J. Morrison, et al. 2007. Loss of Vac14, a regulator of the signaling lipid phosphatidylinositol 3,5-bisphosphate, results in neurodegeneration in mice. *Proc. Natl. Acad. Sci. USA*. 104:17518–17523. doi:10.1073/pnas.0702275104